

IN VIVO EPIGENETIC STUDY OF HISTONE
ACETYLATION ASSOCIATED WITH OBESITY

by

Sheva Naahidi

A thesis
presented to the University of Waterloo
in fulfillment of the
thesis requirement for the degree of
Master of Science
in
Biology

Waterloo, Ontario, Canada, 2007

©Sheva Naahidi, 2007

I hereby declare that I am the sole author of this thesis. This is a true copy of the thesis, including any required final revisions, as accepted by my examiners.

I understand that my thesis may be made electronically available to the public.

Abstract

Post translational modifications in histone proteins are transmissible changes that are not coded for in the DNA sequence itself but have a significant affect in the control of gene expression. Eukaryotic transcription is a regulated process, and acetylation plays a major role in this regulation. Deranged equilibrium of histone acetylation can lead to alteration in chromatin structure and transcriptional dysregulation of genes that are involved in the control of proliferation, cell-cycle progression, differentiation and or apoptosis. Evidence shows that high glucose conditions mimicking diabetes can increase histone acetylation and augment the inflammatory gene expression. Recent advances also highlight the involvement of altered histone acetylation in gastrointestinal carcinogenesis or hyperacetylation in amelioration of experimental colitis. However, the role of histone acetylation under obesity conditions is not yet known. Therefore in the present study, western blot analysis in the liver of Zucker obese versus lean rats was performed to determine the pattern and level of H3 and H4 acetylation (both in nuclear and homogenate fractions) at specific lysine (K) in pathological state of hepatic steatosis The same technique was also applied in the liver of obese rats fed higher amounts of vitamin B6 (OH) versus those fed normal amounts of vitamin B6 (ON) to assess if hyperacetylation can be a protective response to hepatic steatosis. In both experimental models, it was also of interest to elucidate the expression of anti- and pro- apoptotic factor Bcl-2 and Bax in respect to histone acetylation.

It was observed that, in liver homogenate fractions in control animals (LC/OC), there was a higher level of histone H3 acetylation at (K9, K14) and H4 acetylation at K5

in the obese animals. In contrast, the nuclear level of H3 and H4 acetylation at the same lysine residues was considerably higher in the lean and lower in the obese animals. Obese animals contained lower liver preneoplastic lesions as well as liver weight as a result of higher amounts of vitamin B6, had significantly higher H3 acetylation at K9 and K14 and H4 acetylation at K5, in both homogenate and nuclear fractions. However, histone acetylation was not detected for histone H4 at lysine 12 (K12) in either control group (LC/OC) or obese with different B6 diet group (OH/ON). Nevertheless, global histone H3 and H4 acetylation in both homogenate and nuclear fractions, was slightly higher in the lean rats and obese rats fed higher amounts of B6. By using the western blot technique, the level of anti- and pro- apoptotic Bcl-2 and Bax were also evaluated. The moderately higher level expression of anti-apoptotic Bcl2 protein was found in lean animals, whereas the expression of pro-apoptotic Bax was significantly higher in obese animals. Furthermore, anti-apoptotic Bcl2 protein expression was slightly higher in the obese rats fed normal amounts of B6 diet; but, pro-apoptotic Bax was higher in the obese rats fed higher amounts of vitamin B6.

This is the first study which shows that hyperacetylation of histones in liver nuclei can be correlated with amelioration of hepatic steatosis. Histone acetylation and B6 rich diet might be involved in the regulation of biological availability of key apoptotic proteins, which, in turn, can possibly modify the severity of the disease.

Acknowledgments

Throughout my graduate studies, there have been a lot of people who helped me and without their help it would not have been possible for me to finish my project.

I would first like to thank my supervisor, Professor Ranjana P. Bird for providing me with the opportunity to work in her laboratory and for her continuous support throughout the course of my graduate studies.

I gratefully acknowledge my MSc. committee members, Prof. Bernard Duncker and Prof. Mungo Marsden for insightful and thorough comments. I also appreciate their valuable suggestions, time and critical advices.

I am deeply indebted to Dr. Dragana Miskovic for her continuous guidance not only throughout my research but also helping me to analyze, organize, and document my results. This thesis would not have reached a successful completion without her support.

Special thanks go to Prof. Vassili Karanassios, my PhD supervisor, for his special care, and help not only in my seminar and proposal presentation but also in editing and proofreading of my proposal as well as my thesis.

My thanks with love to my mom, Mahin, for giving me love and trust and my brother Shahram who always made me to want to be not only a better student but a better person through my life. I also appreciate my dear sister Shideh for affection and encouragement.

I would like to express my deep appreciation to my reliable and true friend Jeyran Amirloo, who greatly helped me with the organization of my thesis, and was there for me almost every minute of my last week of submission. Thank you both Jean-Luc Orgiazzi for helping me in a software job, and Nafiseh Nafisi my lab mate who made the lab a better place for me to work and helped me during the low times.

The tissues were received from rats that were raised and cared for by Aneta. J. Kular and Erin Burrows, whose collaboration I gratefully acknowledge.

Last, but most importantly, I would like to thank my beloved husband Hamed, Prof. A Hamed Majedi, for his continuous support, engorgement and being there always for me.

Without your support none of these successes would have been possible.

My great and special thanks to my son, Farhan, whom I missed a lot of his beautiful days over my graduate studies, for being a good son and giving me that beautiful smile which promoted me to keep going through difficult times in order to make him a better life.

Table of contents

ABSTRACT	III
ACKNOWLEDGMENTS.....	V
TABLE OF CONTENTS	VII
LIST OF FIGURES.....	IX
LIST OF TABLES.....	XI
ABBREVIATIONS	XII
CHAPTER 1: INTRODUCTION	1
1.1 EPIGENETICS	1
1.2 HISTONES AND CHROMATIN STRUCTURE.....	1
1.3 HISTONE ACETYLATION, DEACETYLATION AND CHROMATIN STRUCTURE	3
1.4 HISTONE ACETYLATION AND GENE TRANSCRIPTION.....	5
1.5 HISTONE ACETYLTRANSFERASE (HAT).....	6
1.5.1 CBP/P300	7
1.5.2 The GNAT Family	7
1.5.3 The MYST Family.....	8
1.5.4 Nuclear Receptor Coactivator.....	8
1.5.5 TAFII250.....	8
1.6 HISTONE ACETYLATION AND DISEASE	9
1.7 HISTONE DEACETYLASES (HDAC).....	10
1.8 HISTONE DEACETYLASE INHIBITORS (HDACI)	10
1.9 APOPTOSIS	12
1.9.1 Bcl-2 Family.....	12
1.10 CHROMATIN REMODELING UNDER HIGH GLUCOSE CONDITION.....	13
1.11 ANTI-INFLAMMATORY EFFECT OF HISTONE HYPERACETYLATION	14
1.12 RAT MODEL OF OBESITY (ZUCKER OBESE RATS).....	15
1.13 OBJECTIVE OF THE RESEARCH	16
CHAPTER 2: MATERIALS AND METHODS	17
2.1 MATERIALS.....	17
2.2 ANIMALS, DIET, BODY WEIGHT AND TERMINATION FOR OBJECTIVE 1.....	17
2.3 ANIMALS, DIET, BODY WEIGHT AND TERMINATION FOR OBJECTIVE 2	18
2.4 SAMPLE PREPARATION FOR <i>IN VIVO</i> ANALYSIS	19
2.4.1 Preparation of Whole Extract from Liver Tissue.....	19
2.4.2 Nuclear Extraction.....	20
2.5 WESTERN BLOT ANALYSIS	21
2.5.1 Protein Assay.....	21
2.5.2 Sodium Dodecyl Sulfate-Polyacrylamide Gel Electrophoresis (SDS-PAGE).....	22
2.5.3 Western Blot	22
2.5.4 Antibody Detection.....	23
2.6 DENSITOMETRY AND STATISTICAL ANALYSIS	24
CHAPTER 3: RESULTS.....	25
3.1 PROTEIN EXPRESSION PATTERN IN CONTROL LIVER TISSUE (LC/OC)	25
3.1.1 Identification of Acetylated Global Histone H3 and H4.....	25
3.1.2 Identification of Specific Lysines Acetylated on Histone H3 and H4	26
3.2 PROTEIN EXPRESSION PATTERN IN OBESE WITH HIGH VITAMIN B6 VS. OBESE WITH NORMAL VITAMIN B6 (OH/ON).....	57
3.2.1 Identification of Global as well as Specific Lysines Acetylated on Histone H3 and H4.....	57
3.3 IDENTIFICATION OF THE LEVEL OF BAX AND BCL-2 PROTEIN EXPRESSION IN LC/OC AND OH/ON GROUP.....	58

CHAPTER 4: DISCUSSION	100
APPENDIX	106
REFERENCES	110

List of Figures

FIGURE 1: SCHEMATIC PRESENTATION OF THE CORE HISTONE PROTEIN.....	3
FIGURE 2: SCHEMATIC PRESENTATION OF CHROMATIN STRUCTURE REGULATING TRANSCRIPTIONAL ACTIVITY.....	4
FIGURE 3: SCHEMATIC REPRESENTATION OF THE EXPERIMENTAL PROTOCOL FOR EFFECT OF SUPPLEMENTARY VITAMIN B6 IN THE ZUCKER OBESE RAT MODEL.....	19
FIGURE 4: WESTERN BLOT ANALYSIS OF HISTONE 3 (GLOBAL HISTONE) HISTONE ACETYLTATION FORM LIVER HOMOGENATES OF ZUCKER RATS.....	27
FIGURE 5: WESTERN BLOT ANALYSIS OF HISTONE 4 (GLOBAL HISTONE) HISTONE ACETYLTATION FROM LIVER HOMOGENATES OF ZUCKER RATS.....	29
FIGURE 6: WESTERN BLOT ANALYSIS OF HISTONE 3 (GLOBAL HISTONE) HISTONE ACETYLTATION FORM LIVER NUCLEAR FRACTIONS OF ZUCKER RATS.....	31
FIGURE 7: WESTERN BLOT ANALYSIS OF HISTONE 4 (GLOBAL HISTONE) HISTONE ACETYLTATION FROM LIVER NUCLEAR FRACTIONS OF ZUCKER RATS.....	33
FIGURE 8: SUMMARY OF NORMALIZED DENSITOMETRY QUANTIFICATION OF LC/OC GLOBAL HISTONE 3 AND 4.....	35
FIGURE 9: WESTERN BLOT ANALYSIS OF HISTONE 3 (LYS 9) HISTONE ACETYLTATION FROM LIVER HOMOGENATES OF ZUCKER RATS.....	37
FIGURE 10: WESTERN BLOT ANALYSIS OF HISTONE 3 (LYS 14) HISTONE ACETYLTATION FROM LIVER HOMOGENATES OF ZUCKER RATS.....	39
FIGURE 11: WESTERN BLOT ANALYSIS OF HISTONE 4 (LYS 5) HISTONE ACETYLTATION FROM LIVER HOMOGENATES OF ZUCKER RATS.....	41
FIGURE 12: WESTERN BLOT ANALYSIS OF HISTONE 4 (LYS 12) HISTONE ACETYLTATION FROM LIVER HOMOGENATES OF ZUCKER RATS.....	43
FIGURE 13: SUMMARY OF NORMALIZED DENSITOMETRY QUANTIFICATION OF HISTONE ACETYLTATION FROM LIVER HOMOGENATES OF ZUCKER RATS.....	45
FIGURE 14: WESTERN BLOT ANALYSIS OF HISTONE 3 (LYS 9) HISTONE ACETYLTATION FROM LIVER NUCLEAR FRACTION OF ZUCKER RATS.....	47
FIGURE 15: WESTERN BLOT ANALYSIS OF HISTONE 3 (LYS 14) HISTONE ACETYLTATION FROM LIVER NUCLEAR FRACTION OF ZUCKER RATS.....	49
FIGURE 16: WESTERN BLOT ANALYSIS OF HISTONE 4 (LYS 5) HISTONE ACETYLTATION FROM LIVER NUCLEAR FRACTION OF ZUCKER RATS.....	51
FIGURE 17: WESTERN BLOT ANALYSIS OF HISTONE 4 (LYS 12) HISTONE ACETYLTATION FROM LIVER NUCLEAR FRACTION OF ZUCKER RATS.....	53
FIGURE 18: SUMMARY OF NORMALIZED DENSITOMETRY QUANTIFICATION OF LIVER NUCLEAR FRACTIONS IN ZUCKER RATS.....	55
FIGURE 19: WESTERN BLOT ANALYSIS OF HISTONE 3 (GLOBAL HISTONE 3) HISTONE ACETYLTATION FROM LIVER HOMOGENATES OF ZUCKER OBESE RATS.....	60
FIGURE 20: WESTERN BLOT ANALYSIS OF HISTONE 4 (GLOBAL HISTONE 4) HISTONE ACETYLTATION FROM LIVER HOMOGENATES OF ZUCKER OBESE RATS.....	62
FIGURE 21: WESTERN BLOT ANALYSIS OF HISTONE 3 (GLOBAL HISTONE) HISTONE ACETYLTATION FROM LIVER NUCLEAR FRACTIONS OF ZUCKER OBESE RATS.....	64
FIGURE 22: WESTERN BLOT ANALYSIS OF HISTONE 4 (GLOBAL HISTONE) HISTONE ACETYLTATION FROM LIVER NUCLEAR FRACTIONS OF ZUCKER OBESE RATS.....	66
FIGURE 23: SUMMARY OF NORMALIZED DENSITOMETRY QUANTIFICATION OF HISTONE ACETYLTATION FROM LIVER HOMOGENATES OF ZUCKER OBESE RATS.....	68
FIGURE 24: WESTERN BLOT ANALYSIS OF HISTONE 3 (LYS 9) HISTONE ACETYLTATION FROM LIVER HOMOGENATES OF ZUCKER OBESE RATS.....	70
FIGURE 25: WESTERN BLOT ANALYSIS OF HISTONE 3 (LYS 14) HISTONE ACETYLTATION FROM LIVER HOMOGENATES OF OBESE ZUCKER RATS.....	72
FIGURE 26: WESTERN BLOT ANALYSIS OF HISTONE 4 (LYS 5) HISTONE ACETYLTATION FROM LIVER HOMOGENATES OF OBESE ZUCKER RATS.....	74
FIGURE 27: WESTERN BLOT ANALYSIS OF HISTONE 3 (LYS 12) HISTONE ACETYLTATION FROM LIVER HOMOGENATES OF OBESE ZUCKER RATS.....	76

FIGURE 28: SUMMARY OF NORMALIZED DENSITOMETRY QUANTIFICATION OF HISTONE ACETYLATION FROM LIVER HOMOGENATES OF OBESE ZUCKER RATS.....	78
FIGURE 29: WESTERN BLOT ANALYSIS OF HISTONE 3 (LYS 9) HISTONE ACETYLATION FROM LIVER NUCLEAR FRACTION OF OBESE ZUCKER RATS.	80
FIGURE 30: WESTERN BLOT ANALYSIS OF HISTONE 3 (LYS 14) HISTONE ACETYLATION FROM LIVER NUCLEAR FRACTION OF OBESE ZUCKER RATS.	82
FIGURE 31: WESTERN BLOT ANALYSIS OF HISTONE 4 (LYS 5) HISTONE ACETYLATION FROM LIVER NUCLEAR FRACTION OF OBESE ZUCKER RATS.	84
FIGURE 32: WESTERN BLOT ANALYSIS OF HISTONE 4 (LYS 12) HISTONE ACETYLATION FROM LIVER NUCLEAR FRACTION OF OBESE ZUCKER RATS.	86
FIGURE 33:SUMMARY OF NORMALIZED DENSITOMETRY QUANTIFICATION OF HISTONE ACETYLATION FROM LIVER NUCLEAR FRACTION OF OBESE ZUCKER RATS.	88
FIGURE 34: WESTERN BLOT ANALYSIS OF ANTI-APOPTOTIC BCL2 PROTEIN EXPRESSION FROM LIVER HOMOGENATES OF ZUCKER OBESE RATS.....	90
FIGURE 35: WESTERN BLOT ANALYSIS OF PROAPOPTOTIC BAX PROTEIN EXPRESSION FROM LIVER HOMOGENATES OF ZUCKER OBESE RATS.....	92
FIGURE 36: WESTERN BLOT ANALYSIS OF ANTI-APOPTOTIC BCL2 PROTEIN EXPRESSION FROM LIVER HOMOGENATES OF OBESE ZUCKER RATS.....	94
FIGURE 37: WESTERN BLOT ANALYSIS OF PROAPOPTOTIC BAX PROTEIN EXPRESSION FROM LIVER HOMOGENATES OF OBESE ZUCKER RATS.....	96
FIGURE 38: SUMMARY OF NORMALIZED DENSITOMETRIC QUANTITATION OF PROTEIN EXPRESSION FROM LIVER HOMOGENATES OF ZUCKER RATS.	98

List of Tables

TABLE 1: OVERVIEW OF HISTONE DEACETYLASE INHIBITORS.....	11
--	----

Abbreviations

Acetylation	AC
Acetyl-Coenzyme A	CoA
Activator of the Thyroid and Retinoic Acid Receptor	ACTR
Apoptotic protease activating factor-1	Apaf-1
Bromodomain	BrD
Chromatin Assembly Factor-1	CAF1
Chromodomains	CHD
CREB binding protein	CBP
Cyclic AMP Response Element Binding Protein	CREB
Cyclooxygenase-2	COX-2
Dithiothreitol	DDT
GCN5-Related N- Acetyltransferases	GNAT
General Transcription Factor	GTF
High Glucose	HG
Histone Acetyltransferases	HAT
Histone Deacetylases	HDAC
Methylation	Me
Monocyte Chemoattractant Protein-1	MCP-1
Monocytic Leukemia Zinc	MOZ
MOZ, YBF2/SAS3, SAS2, Tip60	MYST
Nikotinamideadenine Dinucleotide	NAD
Nuclear Factor κ B	NF- κ B
P300/CBP Associated Factor	PCAF
Parasitophorous Vacuole Membrane	PVM
Phosphorylation	P
Plant Homeodomains	PHD
Rubinstein-Taybi Syndrome	RTS
Reactive Oxygen Spicies	ROS
Silent Information Regulator	Sir2
Sodium Dodecyl Sulfate Polyacrylamide Gel Electrophoresis	SDS-PAGE
Steroid Receptor Coactivator	SRC-1
Suberoyl Bis-Hydroxamic Acid	SBHA
Suberoylanilide Hydroxamic Acid	SAHA
TBP-Associated Factor	TAF
	Tris-Buffered Saline Tween-
TBS-T	20
TNF- α	Tumor necrosis factor α
Transcription Factor	TFs
Trichostatin A	TSA
Ubiquitination	Ub
Zucker Obese	Zk-Ob

Chapter 1:

Introduction

1.1 Epigenetics

Epigenetics is the study of reversible heritable changes in gene function that occur without a change in nucleotide sequence of the DNA; therefore, gene function is not only determined by the DNA code but also by epigenetic phenomena.

Over the past fifteen years, it has been shown that gene expression can be regulated by the proteins called histones, which help packing genomic DNA into the nucleus and also by enzymes that modify both histones and the DNA [1, 2]. The two main mechanisms in the epigenetic regulation of gene expression involve DNA methylation and histone modifications. The study of these mechanisms is important since the change of gene expression is implicated in numerous human disorders and diseases, including obesity, diabetes, cancer and developmental abnormalities [3].

1.2 Histones and Chromatin Structure

In 1884 histones were discovered by Albrecht Kossel. The word “histone” comes from the German word of “Histone”, of uncertain origin and perhaps from Greek word histanai or histos. Until the early 1990s, histones were known just as packing material for nuclear DNA. The regulatory functions of histones were discovered during the early 1990s.

It is now known that histones are small basic architectural proteins of 102-135 amino acids that package the genomic DNA of eukaryotic organism into chromatin which is a dynamic macromolecular complex [4]. The basic repeating units of chromatin, the

nucleosome, is composed of two super helical turns of DNA containing approximately 146 base pairs which wrap around an octamer of the four core histones H2A, H2B, H3, and H4 with the addition of linker DNA and histone H1. H1 determines the level of DNA condensation [5]. These highly conserved histone proteins play an important role in determining the structure and function of chromatin which can be dynamically changed. Chromatin condensation provides an extensive barrier to the nuclear machinery that drives processes such as replication, transcription, or DNA repair; while chromatin decondensation facilitates those processes. Each core histone protein has two domains: a histone fold domain or globular domain, which is involved in histone-histone interactions as well as in wrapping DNA in nucleosomes; and a more flexible and charged amino-terminal 'tail' domain of 25-40 residues [5]. The tail lies on the outside of the nucleosome where it can interact with other regulatory proteins and with DNA. The basic N terminal tails of the core histones are subject to various post-translational modifications. The functional effects of tail modifications are dependent on the specific amino acids that are modified.

The selected amino acid residues of the core histones (H3-H4)₂ tetramer are modified by acetylation (AC), methylation (Me), and phosphorylation (P); and H2A-H2B dimers are modified by acetylation, phosphorylation, ubiquitination (Ub), multiubiquitination, and ADP-ribosylation (Figure 1).

The function of these modifications is the focus of attention due to the possibility that the nucleosome, with its modified tail domains, is not only a packer of DNA but also a carrier of epigenetic information that indicates both how genes are expressed as well as how their expression patterns are maintained from one cell generation to the next. Of

such modifications, acetylation and deacetylation have generated the most interest. Also acetylation was the first modification that had been reported to have correlation with gene activity [7].

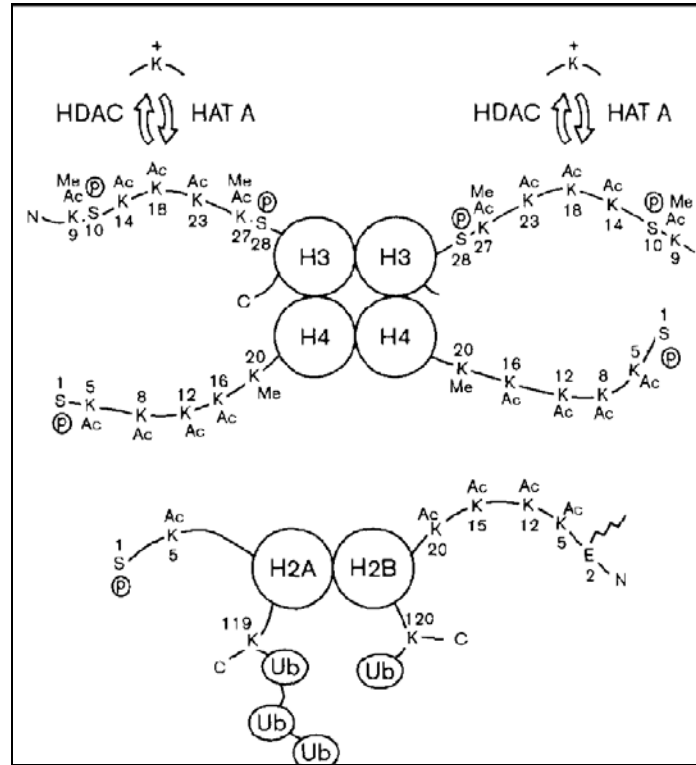


Figure 1: Schematic presentation of the core histone protein.

The enzymes catalyzing reversible acetylation are shown histone acetyltransferase, HAT A; histone deacetylase, HDAC. The core histones are shown as a H2A-H2B dimer and H3-H4 tetramer. Histone modification type are shown as acetylation (Ac), methylation (Me), phosphorylation (P), ubiquitination (Ub), (Davie et. al., 1998)

1.3 Histone Acetylation, Deacetylation and Chromatin Structure

In order to understand the role of acetylation in transcriptional regulation, it would be beneficial to know what structural changes may occur within chromatin as a result of acetylation and/or deacetylation. Currently two theories exist that postulate how histone acetylation may facilitate transcription. The first theory proposes that acetylation neutralizes the positive charge on histones, thereby reducing the affinity between histones and DNA, and relaxing chromatin [8].

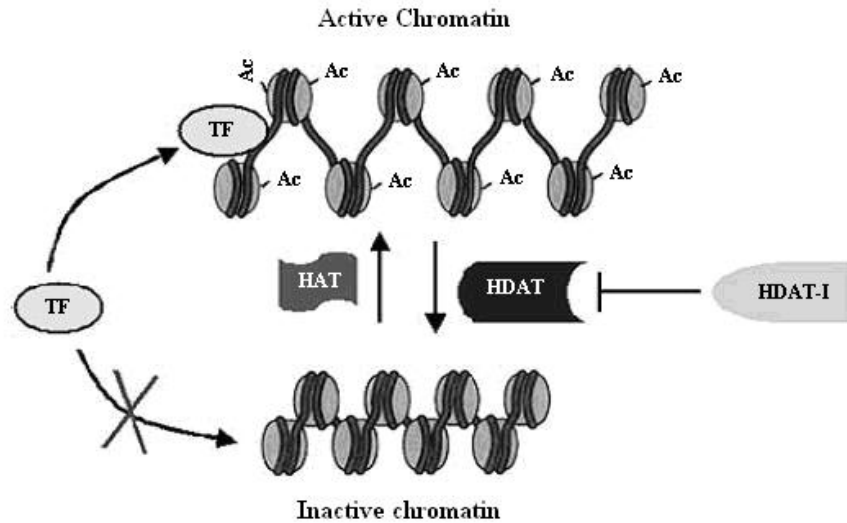


Figure 2: Schematic presentation of chromatin structure regulating transcriptional activity. Histone acetylation (Ac) by acetyltransferase (HAT) makes chromatin to unfold. Therefore transcription factor (TF) can have access to promoter regions of DNA. (E. Di Gennaro *et al.*2004)

Therefore, histone acetylation facilitates the access of Transcription Factors (TFs), and RNA polymerases to promoter regions of DNA [9] and allows transcriptional activation (Figure 2).

A second theory suggests that covalent modification of histones provides an epigenetic marker for gene expression known as “histone code” [10] or ‘epigenetic code’ [12, 13]. In other words the level of affinity of chromatin for chromatin – associated proteins may depend on particular pattern of histone modifications in a cell which determines if chromatin is in an active “euchromatin” or silent “heterochromatin” state.

Histone tails may be involved in the arrangement of higher order chromatin structure and acetylation may facilitate its disruption. Acetylation of H3 and H4 tails, the dominant factor in maintaining chromatin conformation, may disrupt higher order structure rather than destabilize the histone - DNA interaction within the nucleosome [6].

A positive charge on lysine residues of core histones is restored by histone deacetylation, permitting chromatin to change into a highly condensed, transcriptionally silent conformation or heterochromatin. Therefore, in most cases, histone acetylation permits transcription while histone deacetylation represses transcription. Nevertheless, in some cases transcriptional repression occurs as a result of histone acetylation which can be possibly explained by the histone code hypothesis. The balance between histone acetylation/deacetylation is controlled by the competitive activities of 2 superfamilies of enzymes: histone acetyltransferases (HATs) and histone deacetylases (HDACs) [6, 9].

1.4 Histone Acetylation and Gene Transcription

The very first indication of association between acetylation and transcription came from the observation of Allfrey and co-workers who proposed that in actively transcribed regions of chromatin, histones tend to be hyperacetylated, whereas in transcriptionally silent regions histones are hypoacetylated [7]. Many additional studies have solidified this proposal by showing that hyperacetylated core histones are associated with transcriptionally active chromatin [14-18].

Two independent lines of evidence exist that suggest acetylation and transcription may be mechanistically and physiologically related. First, in yeast, altered patterns of transcription due to the mutation of H4 lysine residues have been reported. Those mutations prevented the acetylation of the H4 tail [19]. Second, treatment of mammalian cells with effective inhibitors of histone deacetylase activity, such as trapoxin and trichostatin A, resulted in augmented expression of a diversity of genes [20]. However, after identification of the structure and function of a variety of histone acetyltransferases

and deacetylases the molecular mechanisms of these processes became clearer. The interesting part of these findings is that numerous HATs and HDACs are proteins initially characterized as being involved in transcriptional regulation.

1.5 Histone Acetyltransferase (HAT)

An early indication that histone acetyltransferases (HAT) are involved in transcription came from the discovery of a protein p55 in *Tetrahymena* [21]. P55 is related to yeast protein, GCN5 (transcriptional coactivator/adaptor), and was found to acetylate histones [19]. Currently, numerous co-activator proteins are known to have HAT activity [22]. HAT which links chromatin modification to gene activation, is the catalytic subunit of a multi-subunit protein complex [12] that catalyzes the transfer of an acetyl group from acetyl-CoA to the specific lysine residues on the N-terminal regions of the histones. All HATs contain an acetyltransferase domain, and a shared domain that can be used to group HATs into subfamilies [20]. Sequence analysis of HAT proteins shows that they contain a high sequence similarity within families but little to no sequence similarity between families [21]. Furthermore, each HAT family has a distinct substrate preference, and different families are in different functional contexts. Typically, HATs acetylate global histones or nucleosome substrates. In most cases, the ability to acetylate nucleosome substrates reflects a role for HAT in chromatin modification. The ability of HATs to acetylate only global histones may reflect a role in nucleosome assembly [22].

There have been five families of histone acetyltransferases reported which contain more than twenty enzymes.

1.5.1 CBP/P300

CBP/P300 (**C**REB **B**inding **P**rotein) consists of two highly homologous transcriptional coactivators that participate in many physiological processes, including proliferation, differentiation and apoptosis [23]. The P300/CBP family is found in a variety of multicellular organisms, but it does not exist in yeast. CBP was originally identified as a coactivator for the transcription factor CREB [24, 25] and may be critical for the normal development and functioning of the hematopoietic system [25]. The CBP/P300 family of enzymes is more efficient and has less substrate specificity than the other HAT enzymes since recombinant CBP/P300 has been shown to acetylate all four histones in global-histone form as well as in nucleosomes [24].

Furthermore P300 was isolated as a target of the adenoviral transforming protein E1A [24, 26] which form viral oncoprotein complex that causes a loss of cell growth control, enhances DNA synthesis and blocks cellular differentiation [27].

1.5.2 The GNAT Family

The GNAT (**G**CN5- related **N**-**A**cetyl**T**ransferases) superfamily consists of HAT's that show a sequence and structural similarity to yeast GCN5 [10] 'contains proteins that share one or several conserved sequence motifs [28]. In particular Gcn5 homologues have been identified in a wide range of eukaryotes. Humans express two Gcn5-like proteins including: Gcn5 and PCAF (**p**300/**C**BP **A**ssociated **F**actor) both of which can interact with p300/CBP [29], and have a role in transcriptional regulation and cell cycle control.

1.5.3 The MYST Family

The MYST family is named according to its members, (**M**OZ, **Y**BF2/SAS3, **S**AS2, **T**ip 60). The MYST family of HAT proteins has diverse biological functions in cell-cycle and growth control, transcription activation, positive transcriptional silencing (Sas2 and Sas3) [30], formation of leukemic translocation products (MOZ and TIF2) [31,32], dosage compensation in *Drosophila* (MOF) [33], and DNA repair [34]. The MOZ (**m**onocytic leukemia **z**inc finger protein) is a human proto oncogene that has a homology with yeast Sas3 which is the catalytic subunit of the nucleosomal H3-specific HAT complex, NuA3 [35]. The human MOZ protein stimulates acute myeloid leukaemia AML1-mediated transcription [36].

1.5.4 Nuclear Receptor Coactivator

This family facilitates the assembly of basal transcription factors into a stable pre-initiation complex which in turn stimulates gene expression [37].

Some of the human coactivators such as ACTR, SRC-1 and TIF2, which are involved in certain types of leukemia, can acetylate global or nucleosomal histones H3 and H4 by interacting with nuclear hormone receptors [38, 39].

1.5.5 TAFII250

TAFII250 (**T**BP-**a**ssociated **f**actor) is a subunit of the TFIID complex, a general transcription factor (GTF) that provides a critical first step in transcription initiation.

1.6 Histone Acetylation and Disease

It is hypothesized that different diseases can be the result of hyperacetylation of chromosomal regions that are generally silenced or deacetylation of chromosomal regions that are generally actively transcribed; therefore, alterations of HATs and HDACs at the genomic level disturb the equilibrium of histone acetylation and deacetylation which in turn acts as a key factor in regulating gene expression. Review of some of the diseases associated with aberrant HAT and / or HDACs activity can solidify this hypothesis.

Mutations in the human CBP gene have been reported to be associated with Rubinstein-Taybi syndrome (RTS) which is a developmental haploinsufficiency disorder with an increased risk of cancer development [1, 28, 40].

In human cancer, spontaneously occurring mutations in the P300 gene have been reported [26, 41] which reinforce the idea that indicate ‘P300/CBP activity can be under abnormal control in human disease, particularly in cancer, which may inactivate a p300/CBP tumor-suppressor-like activity [27]’.

PCAF can interact with two important cell cycle regulators: E2F and p53. Transcription factor E2F induces S-phase specific gene expression and is involved in promoting S-phase-entry. In contrast, p53 acts as a tumor suppressor protein by inhibiting cell cycle progression and S-phase entry. Induction of p53 usually leads to post-translational modifications of the protein [42]. Several reports have been shown that acetylation of the C-terminal regulatory domain is involved in regulating activity of p53 [43, 44]. Acetylation of this site is observed after DNA damage *in vivo*, induced p53 and caused cell cycle arrest or apoptosis; therefore, over expression of PCAF can cause growth arrest [28]. On the other hand acetylation of E2F increases the transcriptional

activity of E2F in vivo and stabilizes the E2F protein [28]. Therefore, PCAF can be involved in two opposing scenarios: one is promoting of cell cycle progression by activating E2F, the other is cell cycle arresting by activating p53. Thus, significant effects on cellular proliferation and tumor formation can be the result of PCAF mutation.

1.7 Histone Deacetylases (HDAC)

The identification of several histone deacetylase (HDAC) enzymes [45] whose activities have been correlated with transcriptional repression came almost in parallel to the discovery of HAT enzymes. The histone deacetylases are classified into three classes [45]. Class I contains HDAC 1-3, 8 and 11 which are related to the yeast Rpd.3 histone deacetylases. [45] Class II contains HDAC 4-7, 9 and 10 which are related to the yeast Hda1 histone deacetylases [46]. Class III, is also known as the Sir2 (silent information regulator)-like deacetylases family, consists of 7 genes related to yeast Sir2 and have nikotinamideadenine dinucleotide (NAD)⁺ - dependent deacetylase activity [46].

1.8 Histone Deacetylase Inhibitors (HDACI)

Effective histone deacetylase inhibitors can cause hyperacetylation of nucleosomal histones and histone deacetylation repression [47] which affects cell growth, proliferation, differentiation, and/or apoptosis [1]. HDACI can be divided into four major classes based on their chemical structures (Table 1). Even though, all classes of HDACI promote acetylation, each individual HDACI has a different effect on the stimulation of differentiation and/or apoptosis [48]. Short-chain fatty acids, valproic acid and Sodium butylate, non-specifically react with enzymes and inhibit deacetylation with millimolar

concentration which is a relatively high dose [48, 49]. It is important to note that only these two fatty acids have been approved, so far, for safe clinical use [50]. The hydroxamate class of HDACI, including Trichostatin A (TSA), suberoylanilide hydroxamic acid (SAHA), Suberoyl bis-hydroxamic acid (SBHA), pyroxamide, and Oxamflatin, inhibit deacetylation selectively and are effective at a lower concentration dose (in the micro-nano range) [51]. For example TSA and SAHA stimulate reversibly about 2% of specific gene promoters [52] and induce differentiation both *in vitro* and *in vivo* [53].

The cyclic tetrapeptide class contains Trapoxin, apicidin, and depsipeptide (FR901228). Depsipeptide is a natural product. The trapoxins have been isolated from fungal metabolites as cyclic tetrapeptides and they irreversibly inhibit HDAC. Their inhibitory effects are obtained at nanomolar concentration [51]. The last class of HDACI are composed of synthesized benzamid derivatives MS-275 and CI-994; CI-994 has an effective suppressive activity on cancer cell proliferation [52].

Table 1: Overview of histone deacetylase inhibitors.

	Substance groups	Derivatives
HDAC inhibitors	Short chain fatty acids	Butyrate, valproate
	Hydroxamates	Trichostatin A (TSA), oxamflatin, scriptaid, suberoylanilide hydroxamic acid (SAHA), pyroxamide, NVP-LAQ824, cyclic hydroxamic acid containing peptides (CHAPs)
	Cyclic tetrapeptides	Trapoxins, HC-toxin, chlamydocin, apicidin, depsipeptide (FR901228 or FK228)
	Benzamides	MS-275, N-acetyldinaline (CI-994)
	Sulfonamide anilides	N-2-aminophenyl-3-[4-(4-methyl benzenesulfonylamino)-phenyl]-2-propenamide
	Others	Depudecin

(Mel *et al*, 2004) [11]

1.9 Apoptosis

For the first time, the term “apoptosis” or “program cell death” [53] was proposed by Kerr et al. to describe the “falling off” of leaves from trees [54] which coincides with the morphology of apoptosis. Characteristic features of apoptosis include shrinkage of cells, blebbing of the membrane, condensation of the nucleus and finally formation of apoptotic bodies [55]. Apoptosis plays an important role in various processes such as normal development, differentiation, and homeostasis. Apoptosis is involved in maintaining balance between cell division and cell death (apoptosis) and is an essential key for maintaining of these processes. Therefore, dysfunction or deregulation of the apoptotic program leads to many pathological conditions including cancer [56].

1.9.1 Bcl-2 Family

The Bcl-2 family of proteins is involved in enhancement or suppression of apoptotic pathways by releasing pro- and anti-apoptogenic factors-such as cytochrom *c* from the mitochondria in which caspase activity occurs [57]. Bax, Bad, Bim, Bid, and Bik are pro-apoptotic and Bcl2 and Bcl-xL are anti-apoptotic factors, which together regulate apoptotic pathways. Bcl-2 dimer suppresses the apoptotic pathway by binding to Apaf-1 (**A**poptotic **p**rotease **a**ctivating **f**actor-1) and preventing it from activating caspase-9, whereas Bax dimer causes an influx of ions through mitochondrial membrane and promotes release of cytochrome C into the cytosol which then binds to Apaf-1 and activates the downstream caspase cascade activity. Heterodimerization of anti-apoptotic Bcl-2 proteins, such as Bcl-2, with pro-apoptotic Bax suppresses apoptosis [58]; thus, the ratio of pro-apoptotic Bax to anti-apoptotic Bcl-2 plays an important role in

determination of cell fate. Tumor cells can either be controlled by oncogenes which may be activated on the epigenetic level via histone acetylation or they can contain inactivated tumor suppressor genes which may be silenced via histone deacetylation mechanisms. Therefore, gaining insight into the relationship between apoptosis factors and histone acetylation levels and/or patterns of histone acetylation can give a better understanding of genes controlling cell proliferation and cell death.

1.10 Chromatin Remodeling under High Glucose Condition

Evidence shows that high glucose (HG) conditions, mimicking diabetes, can activate the transcription of nuclear factor Kappa B (NF- κ B) -regulated inflammatory genes [59]. It was shown by *in vitro* experiments with monocyte cell culture that high glucose (HG) conditions lead to the activation of the transcription factor NF- κ B and considerably amplify the expression of a number of inflammatory chemokines and cytokines such as tumor necrosis factor- α (TNF- α), and monocyte chemoattractant protein-1 (MCP-1) [60, 61]. NF- κ B regulates expression of more than 100 genes including inflammatory genes such as TNF- α , and cyclooxygenase-2 (COX-2). NF- κ B is a heterodimer that consists of 65 and 50-kDa subunits (p65 and p50), which is bound to its inhibitor, I κ B, in the cytoplasm. P65 is a key transcription activating component of NF- κ B. Recent studies by F. Miao *et. al* (2004) have shown the occurrence of chromatin rearrangements at the promoters of inflammatory genes *in vivo* in monocytes under diabetic conditions [59]. It was noted that HG culture of monocytes could specifically enhance the recruitment of p65 and coactivator HATs such as CBP and PCAF to the promoters of inflammatory genes (TNF- α , COX-2) as well as an increase in the

acetylation of nucleosomal factors histone H3 lysine 9 (K9), and lysine 14 (K14) and H4 (K5, K8, K12). *In vivo* relevance has been clarified by examining histone acetylation patterns in monocytes from diabetic patients [59]. These results demonstrate high glucose condition mimicking diabetes can have an effect on *in vivo* chromatin remodeling in both cell culture and in patients by increasing acetylation of specific lysine residue from histone 3 and 4 and by activation of transcription factor NF- κ B and HAT at the promoters of inflammatory genes [59].

1.11 Anti-inflammatory Effect of Histone Hyperacetylation

In 2006, the role of acetylation in inflammatory bowel disease was investigated indirectly by evaluating various classes of histone deacetylases (HDAC) inhibitors. In this study, colon-specific anti-inflammatory effects of (HDAC) inhibitors were evaluated for their *in vitro* capacity to suppress cytokine production and to induce apoptosis and histone acetylation in mice, causing colitis [62]. So far, it is known that alteration in gene transcription is a common mechanism of HDAC inhibitors achieved by increasing the accumulation of hyperacetylated histones H3 and H4 which affects chromatin structure and, thereby, the relationship of the nucleosome and the gene promoter elements [63]. It is also known that HDAC inhibitor is associated with a considerable suppression of pro-inflammatory cytokines; therefore, it was proposed that it contains an anti-inflammatory property [64]. Suberyolanilide hydroxamid acid (SAHA) has potent anti-inflammatory activities, both *in vitro* and *in vivo* [64] ; and the anti inflammatory property of HDAC inhibitors are until now restricted just to SAHA and trichostatin A (TSA), both members of the class of hydroxamic acids. Glauben R. *et. al* [62] not only confirmed the anti-

inflammatory properties of HDAC inhibitor, which resulted in a dose-dependent suppression of cytokine synthesis and apoptosis induction, but also announced a dose-dependent increase in histone 3 acetylation at the site of inflammation under VPA treatment [62]. Therefore, in 2006, it was shown that histone hyperacetylation is associated with amelioration of experimental colitis in mice [62]. Even though this study demonstrated that HDAC inhibitors have strong anti-inflammatory effects in experimental colitis caused by hyperacetylation of H3, it still remains to be identified whether the anti-inflammatory efficacy would also reduce the incidence of gastrointestinal malignancies.

1.12 Rat Model of Obesity (Zucker Obese Rats)

Independent or combined actions of genetic and environmental/epigenetic factors can be involved in the development of many diseases including cancer [65]. Appropriate animal models can help us understand chromatin remodeling and the role of environmental factors in multi-step development of cancer. Results obtained from animal studies are a necessary first step in investigations relevant to the human population. In Canada and many other countries, obesity is one of the important public health problems and it is increasing in both young and adult populations [66]. Obesity is a premorbid condition resulting from either lifestyle factors or genetic [67]. Zucker obese animals have hyperglycemia, hyperinsulinemia, hyperphagia, and hypercholesterolemia [65]. They contain a sustained inflammatory state as well as an increased sensitivity to colon cancer [66, 68]. In addition Zucker obese rats have enlarged liver and also exhibit hepatic steatosis (fatty liver) in their adulthood [69] compared to their lean counterpart. However,

hepatic steatosis in obese rats is similar to those noted in obese humans. Zucker lean counterparts are considered as normal individuals. In a recent study conducted by A. Kular, in our laboratory, it was noted that a high B6 diet reduced liver weight as well as the number of preneoplastic lesions in the Zucker obese rats. It has been suggested that a high B6 could serve as an antioxidant and it could reduce the levels of oxidative stress markers.

Therefore, all of the above information made Zucker rats to be an excellent experimental model to test present study. To meet the overall objective of this project two studies performed. In the following section, the both objectives of this work will be described and the studies performed to meet each objective will be outlined.

1.13 Objective of the Research

The overall objective of this research was to elucidate the pattern and level of H3 and H4 acetylation (both in nuclear and homogenate fractions) in pathological state of hepatic steatosis and determine if hyper-acetylation can be a protective response to hepatic steatosis. It was also of interest to assess the expression of anti- and pro-apoptotic factor Bcl-2 and Bax.

In the present study, it is hypothesized that hyperglycemic and pro-inflammatory conditions in Zucker obese rats will have strong effect on histone acetylation and that tissue extracted from Zucker obese rats would have increased histone acetylation.

Zucker obese rat model and western blot assay were effectively used to demonstrate, for the first time, the effect of histone acetylation in the pathogenesis of hepatic steatosis associated with obesity.

Chapter 2:

Materials and Methods

2.1 Materials

To meet the objectives mentioned above, tissues were obtained from previous studies conducted in our lab. A brief description of experimental approaches and methodology are described below.

Unless otherwise stated, all chemicals, reagents, monoclonal Anti- α -tubulin antibody and β -actin were purchased from Sigma Chemical Co., (Ottawa, Ontario). Some of the primary antibodies were purchased from Upstate Biotechnology (Now part of Millipore corporation, Billerica, MA), all others antibodies were from Santa Cruz Biotechnology (Santa Cruz, CA).

2.2 Animals, Diet, Body Weight and Termination for Objective 1

Twelve female rats [6 Zk-Ob (fa/fa) and 6 Zk-Ln (Fa/Fa)], at the age of 28 days were purchased from Charles River Breeding Laboratories (Montreal, CA). Animals were housed in polypropylene cages lined with woodchip bedding and stainless steel wire mesh lids in the Biology department animal facility. Environmental conditions were controlled for climate and temperature with 12 h light/12 h dark cycle. All animals were cared for according to guidelines of the Canadian council on animal care and the office of Research Ethics, University of Waterloo (AUPP: 04-17).

Experimental diet was based on a low fat diet semi-synthetic AIN-93G standard diet formula with 5% corn oil by weight. Twice a week diets were prepared. Every day food cups were filled and food intake was monitored. Body weights were monitored

weekly from the initial ten weeks of the study and at termination day. Upon the end of an experimental period, at the tenth week, animals were terminated by CO₂ asphyxiation. As a general observation any pathological abnormality was recorded. Weights of liver, kidney, spleen, and heart were recorded for both lean and obese rats, and then samples were frozen for future biochemical analysis at -80°C.

2.3 Animals, Diet, Body Weight and Termination for Objective 2

Fifty two female rats [30 Zk-Ob (fa/fa) and 22 Zk-Ln (Fa/Fa)], at the age of 6 weeks were purchased from Charles River Breeding Laboratories (Montreal, CA). Animals were housed in polypropylene cages lined with woodchip bedding and stainless steel wire mesh in the animal facility. Environmental conditions were controlled for climate and temperature with 12 h light/12 h dark cycle. All animals were cared according to guidelines of the Canadian Council on Animal Care and the Office of Research Ethics, University of Waterloo, (AUPP: 04-17).

Experimental diet was based on a low fat diet semi-synthetic AIN-93G standard diet formula with 5% corn oil by weight. Food cups were filled every day with fresh diet. One animal group received a low fat diet containing the recommended amount of vitamin B6 for comparison and investigation of the effect of high B6 on acetylation pattern, the other group of Zucker obese rat was fed a diet containing five times the recommended amount of vitamin B6 (7mg versus 35mg/kg of diet).

Following a two week period which included feeding of the experimental diet, animals were subcutaneously injected with the colon specific carcinogen, AOM, diluted in 0.9% saline at a dose of 10 mg/kg body weight. The animals received a second

injection, two weeks after the first one. Animals were given free access to the experimental diets during and after the injection period. Body weights were monitored weekly for 6 weeks after the final AOM injection and at termination. A summary of the study design is detailed in Figure 3.

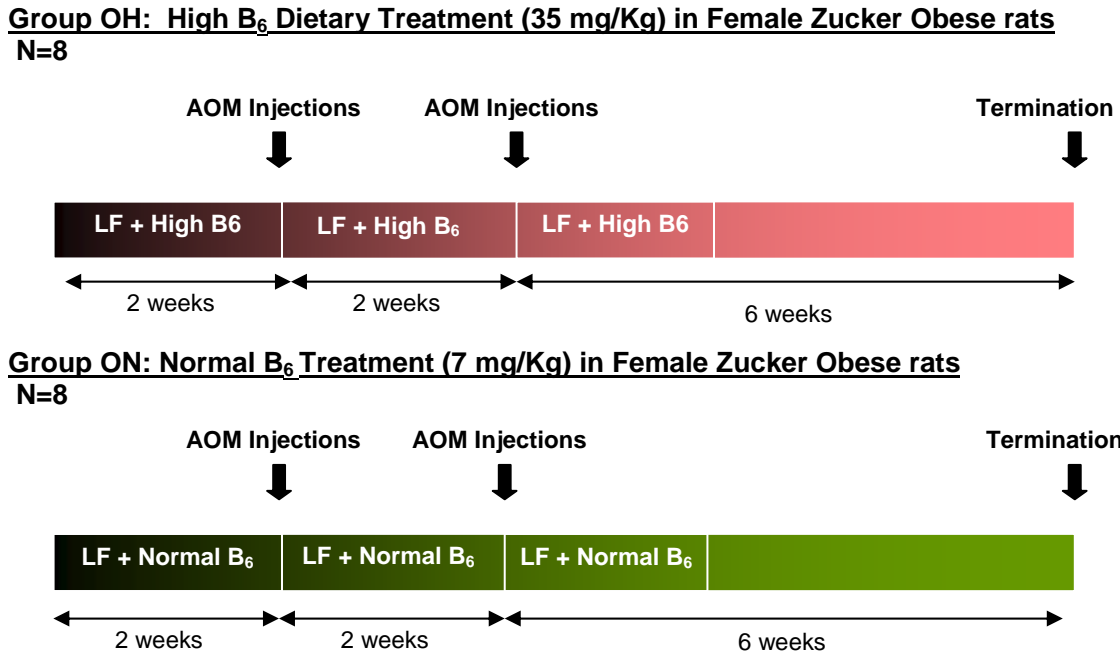


Figure 3: Schematic representation of the experimental protocol for effect of supplementary vitamin B₆ in the Zucker obese rat model.

2.4 Sample Preparation for *In vivo* Analysis

2.4.1 Preparation of Whole Extract from Liver Tissue

One gram of Zucker rat liver was diced and mixed with 4 mL of ice-cold RIPA buffer (50 mM Tris-HCl, 1% NP-40, 0.25% Sodium deoxycholate, 150 mM NaCl, 1 mM EDTA, 1 mM NaF) and freshly added protease inhibitors (1 µg/mL of Aprotinin,

Leupeptin, Trypsin Inhibitor, Sodium Orthovanadate). This mixture was homogenized with PT2100 Polytron homogenizer and transferred into microcentrifuge tubes.

Cell debris and lipids were removed through centrifugation at 15krpm for 20 min at 4°C. The middle layer of this lysate was collected into pre-chilled Eppendorf tubes and stored in -80°C freezer. Equal amount of protein were used for western blot analysis.

2.4.2 Nuclear Extraction

Nuclear Fraction from liver tissue was collected using nuclear extract kit (Active motif, Carlsbad, CA) according to the manufacturer's protocol. The 1X hypotonic buffer and 10mM DTT were made out of 10X hypotonic buffer and 1M DTT respectively. One gram of liver from each group was chopped and mixed with 3 ml of 1X hypotonic buffer, 3µl of 1M DTT and 3µl of provided Detergent. This mixture was homogenized with a PT2100 Polytron homogenizer and incubated for 15 minutes on ice. After incubation, cells were centrifuged at 850 x g for 10 minutes at 4°C and the supernatant was collected. At this point, most of the cells were not yet lysed. Therefore 1ml of 1X hypotonic buffer was again added to the each remaining pellet and vortexed until dissolved, then incubated for 15 minutes on ice. 50 µl detergent was added to each and then vortexed at highest setting. Then suspensions were centrifuged at 14,000 x g for 30 second in a microcentrifuge pre-cooled to 4°C. Tubes were placed on ice while the supernatant (cytoplasmic fractions) was mixed with the supernatant that earlier had been collected and was then aliquoted and stored at -80°C. Remaining pellets each were resuspended in 100 µl of Complete Lysis Buffer (10 µl of 10 mM DTT, 89 µl of lysis Buffer, 1µl of Protease Inhibitor Cocktail) and vortexed at the highest setting for 10

seconds. The Eppendorf tubes containing this mixture were laid horizontally on ice in an ice bucket and were rocked on a rocking platform at maximum speed for 30 minutes. Centrifugation at 14,000 x g for 10 minutes at 4°C was again applied. Supernatants (nuclear fraction) were aliquoted in pre-chilled tubes and stored at -80°C for further analysis. The purity of nuclear fractions was checked by probing with anti-tubulin antibody which is a cytosolic protein.

2.5 Western Blot Analysis

2.5.1 Protein Assay

Bradford Assay was used to determine the concentration of protein. A standard curve was plotted using several known concentration of bovine serum albumin (BSA). The standards were mixed with Bradford reagent (10% CBB G-250, 85% phosphoric acid, and 5% ethanol) in 1:50 dilution. Duplicates of each protein sample were assayed in a 96 well plate; after 5 minutes of incubation the plates were measured with Bio-Rad 3550-UV Micro plate Reader at 595 nm.

Once the absorbance readings were recorded, a standard curve was plotted using the concentration on the x-axis and the absorbance on the y-axis. The program Excel provided an equation, which was then used to determine the concentration of unknown proteins. With the other words BSA standards were used to construct a standard curve that was used to determine the concentration of each protein sample.

2.5.2 Sodium Dodecyl Sulfate-Polyacrylamide Gel Electrophoresis (SDS-PAGE)

Equal amount of 2X SDS Laemmli buffer (Sigma Chemical) and protein sample were mixed and boiled for 5 min at 90°C. Protein bands were analyzed by sodium dodecyl sulfate polyacrylamide gel electrophoresis (SDS-PAGE). The 12% resolving gel was made with Acrylamide-Bis (30% T, 2.67% C) (Bio-Rad Laboratories Ltd, Canada), 1.5 M Tris-HCL (pH 8.8), 10% SDS (Fisher Scientific), 10% Ammonium persulphate, and 0.05% TEMED (Bio-Rad Laboratories Ltd, Canada). The 4% stacking gel was made of using all of the above, but the Tris-HCL buffer was 0.5 M with pH 6.8. Mini-Protein® II gel apparatus (Bio-Rad Laboratories Ltd, Canada) was used to run the gels followed by the staining with Coomassie blue G-250 (J. T. Chemical Co, NJ, USA). Furthermore, similar gels were transferred directly to PVDF membranes in order to detect the bands with specific antibodies.

2.5.3 Western Blot

First, the optimal amount of protein for loading was determined. Protein samples were subjected to 12% SDS-PAGE as discussed in section 2.5.2.

Equal amounts of proteins were separated by SDS-PAGE at 120V for 120 min. A molecular weight marker was loaded in all gels. After separation, proteins were transferred onto 0.45 µm PVDF membranes (Pall Corp. FI, USA). Membranes were presoaked first in methanol for 15 minutes and then in transfer buffer for 1 hour before using the Trans-Blot Semi-Dry transfer cell (Bio-Rad Laboratories Ltd, Canada). Then, the protein gels were placed on the top of a thick Sponge (Bio-Rad Laboratories Ltd,

Canada), onto the anode platform of the Semi-dried system. The PVDF membranes were placed directly onto the gels and another sponge was placed on the membranes. A test-tube was rolled over the thick sponge to get rid of the bubbles. The proteins were then transferred to the PVDF membrane at 20V for 32 minutes. Then gels were stained with Coomassie Brilliant Blue in order to see if proteins properly separated. The PVDF membranes with transferred protein were blocked with TBS-T containing 5% skim milk powder for 2-3 hours at room temperature in order to block the non-specific proteins binding. Then blots were probed with primary antibody in an appropriate dilution for 1.5 hour at room temperature followed by overnight incubation at 4°C. The next day, immunoblots were rocked for another half an hour and then washed with TBS-T (Tris-Buffered Saline Tween-20) four times each 10 minutes. Then membranes were incubated with an appropriate HRP-labeled polyclonal goat anti-rabbit, secondary antibody, in a dilution of 1/5000 in 5% blocking solution for 2 hours. Subsequently, the membranes were washed four times in TBS-T, for 10 minutes each.

2.5.4 Antibody Detection

An ECL plus western blot analysis detection kit was used according to Manufacturer's protocol (Amersham Biosciences Canada, GE Healthcare Bio-Sciences Inc., Quebec, Canada) to discern bound antibody. Detection solution A and B were mixed in a ratio of 40:1, then, blots were incubated for 5 minutes, and detected using X-ray film (Fisher Scientific Company, Ottawa, ON, Canada). The film was exposed for 10 seconds, depending on the intensity of the band, the second film was exposed either for a longer or

shorter period of time. Equal loading of each gel was verified by comparison with the immunoblotting of beta-actin.

2.6 Densitometry and Statistical Analysis

Densitometry analysis was performed using a Visible Imaging System equipped with AlphaEaseFC software (Alpha Innotech, San Leandro, CA). The data obtained were analyzed statistically using SPSS software (SPSS Inc. Headquarters, Chicago, IL). A comparison between the groups of interest was performed by descriptive analysis. All values are means \pm s.e.; and differences were determined at a significance level of $P < 0.05$ as determined by Independent-Samples T-test.

Chapter 3:

Results

3.1 Protein Expression Pattern in Control Liver Tissue (LC/OC)

Western blots were performed to assess relative whole homogenate and nuclear extract protein levels of H3 and H4 acetylated at specific lysine residues. A comparison of obese and lean rats is demonstrated below.

3.1.1 Identification of Acetylated Global Histone H3 and H4

The importance of altered global histone H4 acetylation levels in gastrointestinal carcinogenesis [70] as well as human gastric adenomas and carcinomas has been studied [71]. We therefore wanted to determine if the level of global histone H3 and H4 acetylation is different in obese rats which contained sustained inflammatory state and more sensitivity to colon cancer in compare with their lean counterparts. In order to demonstrate this, western blot assay was performed with anti-acetylated histone H3 and H4 antibodies to determine global acetylation status of histones. The level of acetylated global histone H3 & H4 expression is shown to be slightly reduced in both homogenate and nuclear fractions in obese liver in comparison with their lean counterparts (summary is in figure 8). This is supported by data showing that the level of global histone H4 acetylation reduced in colorectal cancer [71]. A similar reduction of the total amount of acetylated histone H4 with association of tumorigenesis in gastric cancer has been also reported [70]. From these observations, it appears possible that reduced levels of global histone acetylation may possibly participate in sensitivity of obese rats to colon cancer.

3.1.2 Identification of Specific Lysines Acetylated on Histone H3 and H4

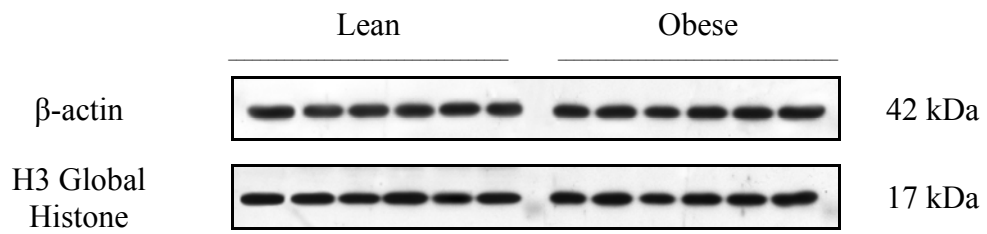
Changes in the level of histones H3 and H4 acetylation at specific lysine residues in several disease such as diabetes and colitis [59,62] shows the importance of specific patterns of histone acetylation at lysine residues for the final outcome of gene expression. Since Zucker obese rats are also known for having hyperglycemia and hepatic steatosis we wanted to examine which specific lysine residue of histone H3 and H4 are acetylated and to compare with their lean counterparts to determine if there is a difference in the level of acetylated histones at specific lysine residues (K). By using anti-acetylated antibodies for histone H3 at K9 & K14 and for H4 at K5 & K12 the level of acetylation in homogenate fraction as well as nuclear fractions in Zucker obese liver was examined. In homogenate fractions, obese rats had a higher level of acetylation in H3 K9, and K14 as well as H4 K5, (summary is in figure 13) suggesting probably higher amount of histones need to go inside the nucleus for chromatin assembly in obese animals.

In obese, in compare with their lean, nuclear fractions, a significantly decreased level of acetylation in H3 K9, & K14 as well as H4 K5 was observed (summary is in figure 18). One possibility can be related to excess of HDAC which can elicit dynamic alterations in HAT to HDAC activities which in turn decrease acetylation level. However, no acetylation was detected for H4 K12 in both homogenate and nuclear fractions (Figure 12 and 17 respectively). These data suggest that acetylation at these sites may be important to the transcriptional activation of some genes such as TNF- α which can play a role in obesity conditions. In addition these differences between acetylation levels of obese verses lean also may indicate a novel critical level of regulation at the level of chromatin. An extensive discussion on this topic is presented later.

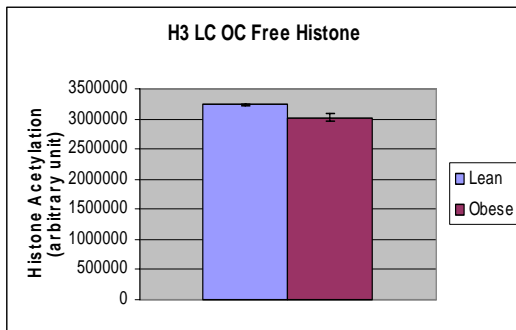
Figure 4: Western Blot Analysis of Histone 3 (Global Histone) Histone Acetylation form Liver Homogenates of Zucker rats

Histone 3 (H3) was analyzed by Western blot analysis as described in Materials and Methods 50 µg of liver Protein Samples was separated by 12% SDS-PAGE gel and transferred onto PVDF membranes. The membrane was cut and probed with primary anti-histone 3 and β-actin separately at a final dilution of 1:500 and 1:5000 respectively. Then secondary antibody (a goat anti-rabbit HRP conjugated) and (a goat anti-mouse HRP conjugated) at a final dilution of 1:2500 and 1:5000 for histone and β-actin was used respectively. The blots were exposed by ECL Plus substrate and developed on X-Ray film. (A) Representative western blots of H3 and β-actin using 50 µg of liver protein from Zucker Obese (Ob) and Lean (Ln) rats. (B) shows densitometric quantitation $p < 0.05$ as determined by Independent-Samples T-test. Bar graph represents level of H3 protein of the relative intensities of H3 bands. The standard deviations of the experiment for each group of 6 animals are shown on the bars as determined by descriptive analysis. (C) shows normalized densitometric quantitation $p < 0.05$ as determined by Independent-Samples T-test. Bar graph represents level of H3 protein of the relative intensities of H3 bands normalized to β-actin. The standard deviations of the experiment for each group of 6 animals are shown on the bars as determined by descriptive analysis.

(A)



(B)



(C)

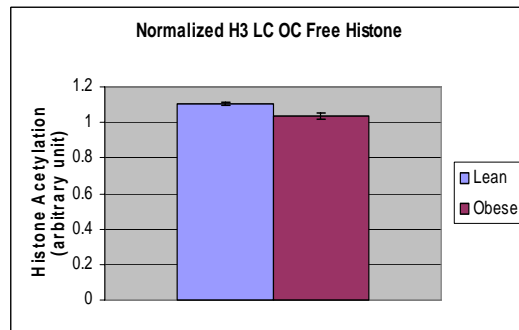
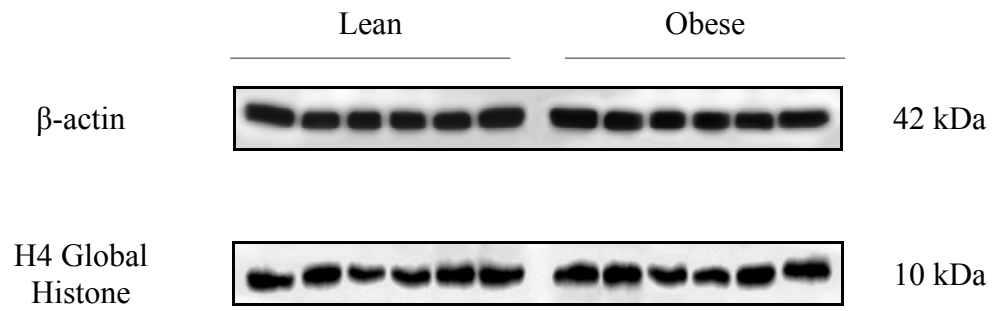


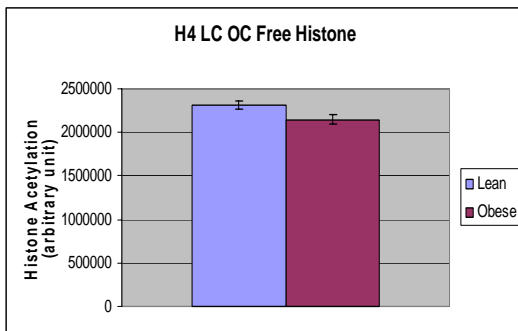
Figure 5: Western Blot Analysis of Histone 4 (Global Histone) Histone Acetylation from Liver Homogenates of Zucker Rats.

Histone 4 (H4) was analyzed by Western blot analysis as described in Materials and Methods 50 µg of liver Protein Samples was separated by 12% SDS-PAGE gel and transferred onto PVDF membranes. The membrane was cut and probed with primary anti-histone 4 and β-actin separately at a final dilution of 1:500 and 1:2500 respectively. Then secondary antibody (a goat anti-rabbit HRP conjugated) and (a goat anti-mouse HRP conjugated) at a final dilution of 1:5000 and 1:2500 for histone and β-actin was used respectively. The blots were exposed by ECL Plus substrate and developed on X-Ray film. (A) Representative western blots of H4 and β-actin using 50 µg of liver protein from Zucker Obese (Ob) and Lean (Ln) rats. (B) shows densitometric quantitation $p < 0.05$ as determined by Independent-Samples T-test. Bar graph represents level of H4 protein of the relative intensities of H4 bands. The standard deviations of the experiment for each group of 6 animals are shown on the bars as determined by descriptive analysis. (C) shows normalized densitometric quantitation $p < 0.05$ as determined by Independent-Samples T-test. Bar graph represents level of H4 protein of the relative intensities of H4 bands normalized to β-actin. The standard deviations of the experiment for each group of 6 animals are shown on the bars as determined by descriptive analysis.

(A)



(B)



(C)

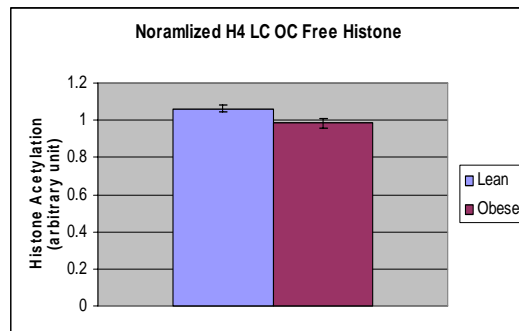
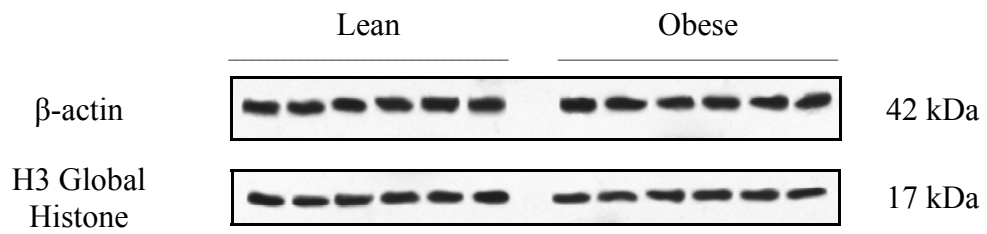


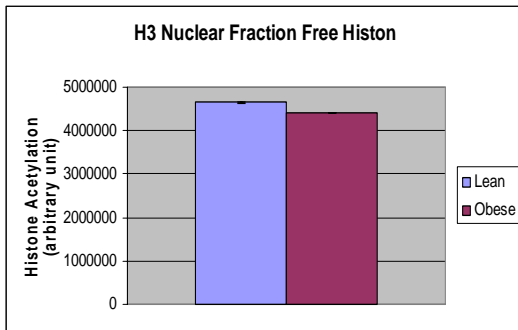
Figure 6: Western Blot Analysis of Histone 3 (Global Histone) Histone Acetylation form Liver Nuclear Fractions of Zucker rats

Histone 3 (H3) was analyzed by Western blot analysis as described in Materials and Methods 50 µg of liver Protein Samples was separated by 12% SDS-PAGE gel and transferred onto PVDF membranes. The membrane was cut and probed with primary anti-histone 3 and β-actin separately at a final dilution of 1:500 and 1:5000 respectively. Then secondary antibody (a goat anti-rabbit HRP conjugated) and (a goat anti-mouse HRP conjugated) at a final dilution of 1:2500 and 1:5000 for histone and β-actin was used respectively. The blots were exposed by ECL Plus substrate and developed on X-Ray film. (A) Representative western blots of H3 and β-actin using 50 µg of liver protein from Zucker Obese (Ob) and Lean (Ln) rats. (B) shows densitometric quantitation $p < 0.05$ as determined by Independent-Samples T-test. Bar graph represents level of H3 protein of the relative intensities of H3 bands. The standard deviations of the experiment for each group of 6 animals are shown on the bars as determined by descriptive analysis. (C) shows normalized densitometric quantitation $p < 0.05$ as determined by Independent-Samples T-test. Bar graph represents level of H3 protein of the relative intensities of H3 bands normalized to β-actin. The standard deviations of the experiment for each group of 6 animals are shown on the bars as determined by descriptive analysis.

(A)



(B)



(C)

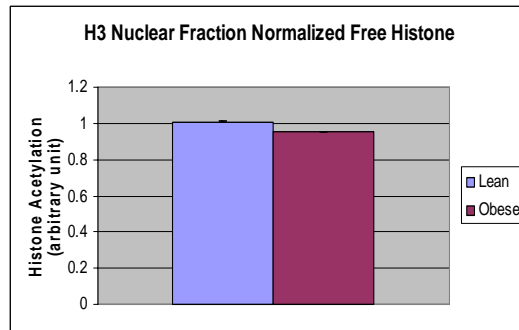
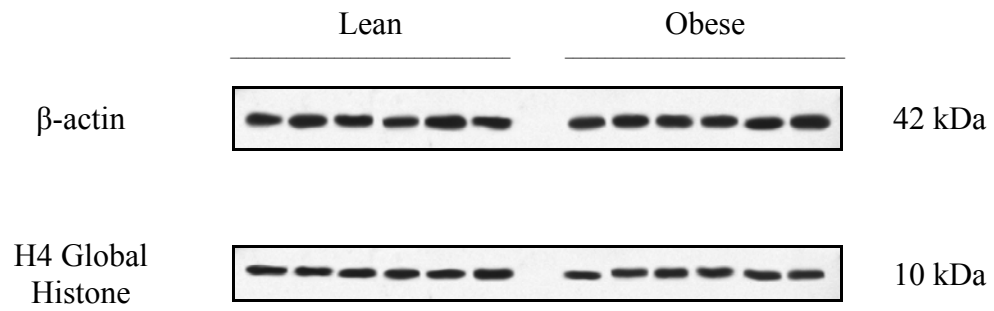


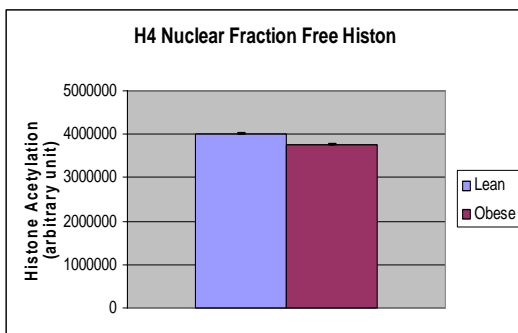
Figure 7: Western Blot Analysis of Histone 4 (Global Histone) Histone Acetylation from Liver Nuclear Fractions of Zucker Rats.

Histone 4 (H4) was analyzed by Western blot analysis as described in Materials and Methods 50 µg of liver Protein Samples was separated by 12% SDS-PAGE gel and transferred onto PVDF membranes. The membrane was cut and probed with primary anti-histone 4 and β-actin separately at a final dilution of 1:500 and 1:2500 respectively. Then secondary antibody (a goat anti-rabbit HRP conjugated) and (a goat anti-mouse HRP conjugated) at a final dilution of 1:5000 and 1:2500 for histone and β-actin was used respectively. The blots were exposed by ECL Plus substrate and developed on X-Ray film. (A) Representative western blots of H4 and β-actin using 50 µg of liver protein from Zucker Obese (Ob) and Lean (Ln) rats. (B) shows densitometric quantitation $p < 0.05$ as determined by Independent-Samples T-test. Bar graph represents level of H4 protein of the relative intensities of H4 bands. The standard deviations of the experiment for each group of 6 animals are shown on the bars as determined by descriptive analysis. (C) shows normalized densitometric quantitation $p < 0.05$ as determined by Independent-Samples T-test. Bar graph represents level of H4 protein of the relative intensities of H4 bands normalized to β-actin. The standard deviations of the experiment for each group of 6 animals are shown on the bars as determined by descriptive analysis.

(A)



(B)



(C)

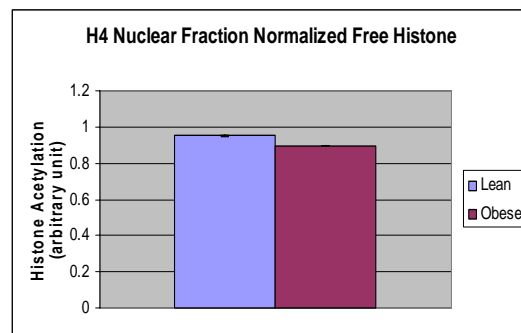
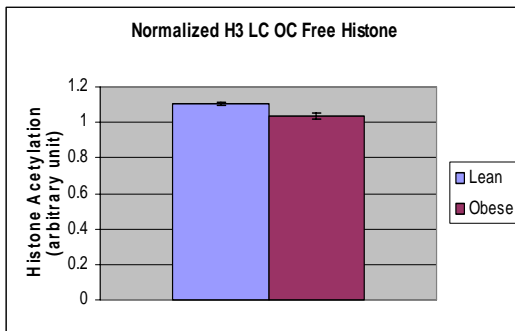


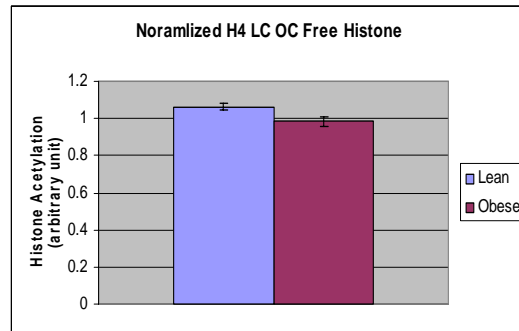
Figure 8: Summary of normalized densitometry quantification of LC/OC Global Histone 3 and 4 acetylation

(a) Histone 3 Acetylation form Liver Homogenates of Zucker rats (b) Histone 4 Histone Acetylation form Liver Homogenates of Zucker rats (c) Histone 3 Histone Acetylation form Liver Nuclear Fractions of Zucker rats (d) Histone Acetylation form Liver Nuclear Fractions of Zucker rats

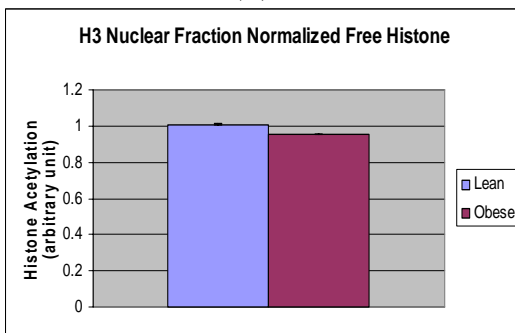
(A)



(B)



(C)



(D)

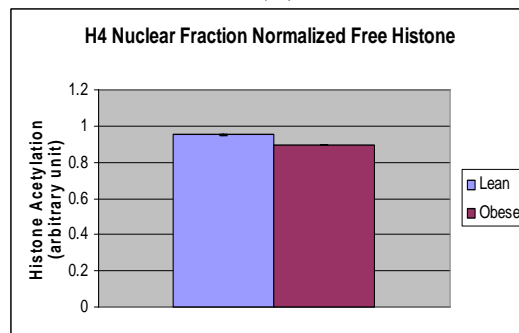
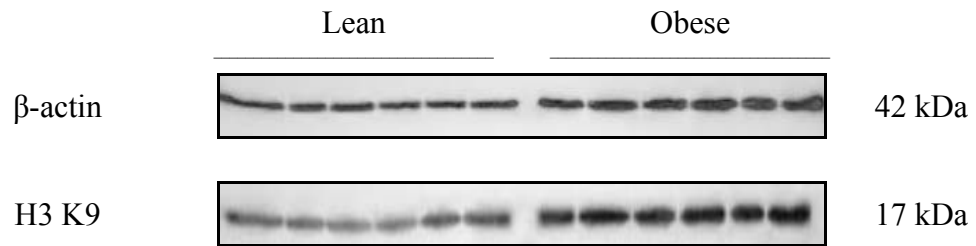


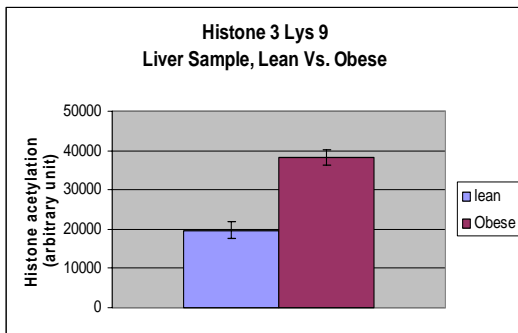
Figure 9: Western Blot Analysis of Histone 3 (Lys 9) Histone Acetylation from Liver Homogenates of Zucker Rats.

Histone 3 Lys 9 was analyzed by Western blot analysis as described in Materials and Methods 50 μ g of liver Protein Samples was separated by 12% SDS-PAGE gel and transferred onto PVDF membranes. The membrane was cut and probed with primary anti-histone 3 Lys 9 and β -actin separately at a final dilution of 1:7500 and 1:10000 respectively. Then secondary antibody (a goat anti-rabbit HRP conjugated) and (a goat anti-mouse HRP conjugated) at a final dilution of 1:5000 and 1:10000 for histone and β -actin was used respectively. The blots were exposed by ECL Plus substrate and developed on X-Ray film. (A) Representative western blots of H3 Lys 9 and β -actin using 50 μ g of liver protein from Zucker Obese (Ob) and Lean (Ln) rats. (B) shows densitometric quantitation $p < 0.05$ as determined by Independent-Samples T-test. Bar graph represents level of H3 Lys 9 protein of the relative intensities of H3 Lys 9 bands. The standard deviations of the experiment for each group of 6 animals are shown on the bars as determined by descriptive analysis. (C) shows normalized densitometric quantitation $p < 0.05$ as determined by Independent-Samples T-test. Bar graph represents level of H3 Lys 9 protein of the relative intensities of H3 Lys 9 bands normalized to β -actin. The standard deviations of the experiment for each group of 6 animals are shown on the bars as determined by descriptive analysis.

(A)



(B)



(C)

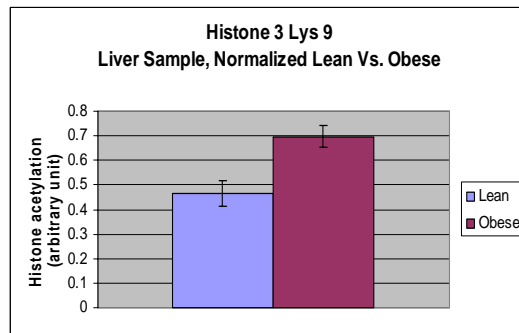
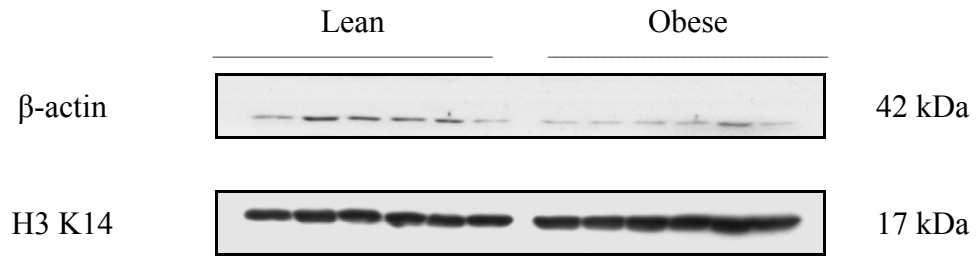


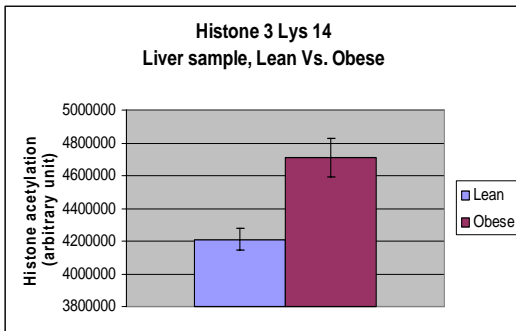
Figure 10: Western Blot Analysis of Histone 3 (Lys 14) Histone Acetylation from Liver Homogenates of Zucker Rats.

Histone 3 Lys14 was analyzed by Western blot analysis as described in Materials and Methods 50 μ g of liver Protein Samples was separated by 12% SDS-PAGE gel and transferred onto PVDF membranes. The membrane was cut and probed with primary anti-histone 3 Lys 14 and β -actin separately at a final dilution of 1:2500 and 1:20000 respectively. Then secondary antibody (a goat anti-rabbit HRP conjugated) and (a goat anti-mouse HRP conjugated) at a final dilution of 1:5000 and 1:20000 for histone and β -actin was used respectively. The blots were exposed by ECL Plus substrate and developed on X-Ray film. (A) Representative western blots of H3 Lys 14 and β -actin using 50 μ g of liver protein from Zucker Obese (Ob) and Lean (Ln) rats. (B) shows densitometric quantitation $p < 0.05$ as determined by Independent-Samples T-test. Bar graph represents level of H3 Lys 14 protein of the relative intensities of H3 Lys 14 bands. The standard deviations of the experiment for each group of 6 animals are shown on the bars as determined by descriptive analysis. (C) shows normalized densitometric quantitation $p < 0.05$ as determined by Independent-Samples T-test. Bar graph represents level of H3 Lys 14 protein of the relative intensities of H3 Lys 14 bands normalized to β -actin. The standard deviations of the experiment for each group of 6 animals are shown on the bars as determined by descriptive analysis.

(A)



(B)



(C)

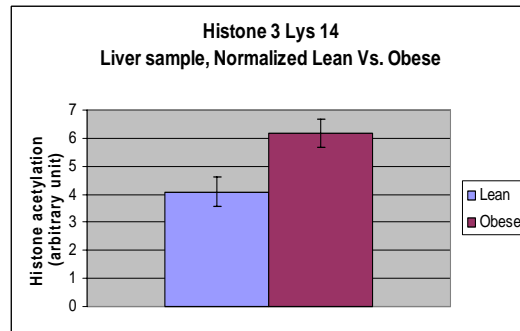
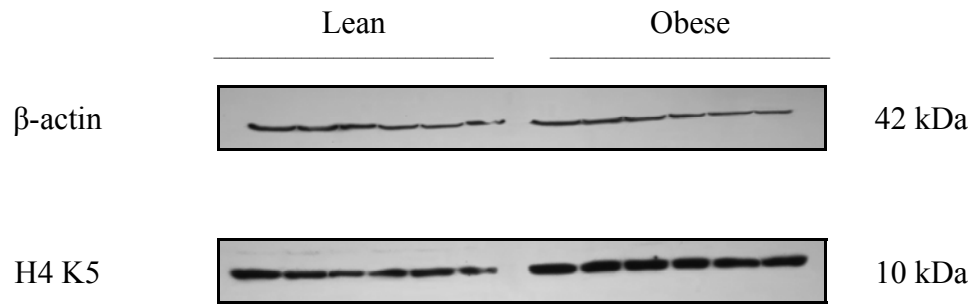


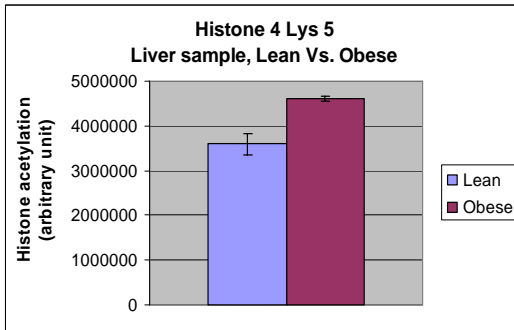
Figure 11: Western Blot Analysis of Histone 4 (Lys 5) Histone Acetylation from Liver Homogenates of Zucker Rats.

Histone 4 Lys 5 was analyzed by Western blot analysis as described in Materials and Methods 50 μ g of liver Protein Samples was separated by 12% SDS-PAGE gel and transferred onto PVDF membranes. The membrane was cut and probed with primary anti-histone 4 Lys 5 and β -actin separately at a final dilution of 1:1000 and 1:10000 respectively. Then secondary antibody (a goat anti-rabbit HRP conjugated) and (a goat anti-mouse HRP conjugated) at a final dilution of 1:5000 and 1:10000 for histone and β -actin was used respectively. The blots were exposed by ECL Plus substrate and developed on X-Ray film. (A) Representative western blots of H4 Lys 5 and β -actin using 50 μ g of liver protein from Zucker Obese (Ob) and Lean (Ln) rats. (B) shows densitometric quantitation $p < 0.05$ as determined by Independent-Samples T-test. Bar graph represents level of H4 Lys 5 protein of the relative intensities of H4 Lys 5 bands. The standard deviations of the experiment for each group of 6 animals are shown on the bars as determined by descriptive analysis. (C) shows normalized densitometric quantitation $p < 0.05$ as determined by Independent-Samples T-test. Bar graph represents level of H4 Lys 5 protein of the relative intensities of H4 Lys 5 bands normalized to β -actin. The standard deviations of the experiment for each group of 6 animals are shown on the bars as determined by descriptive analysis.

(A)



(B)



(C)

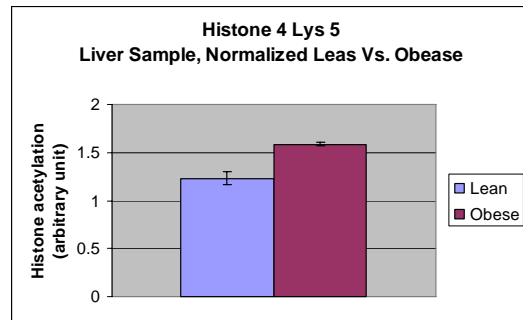


Figure 12: Western Blot Analysis of Histone 4 (Lys 12) Histone Acetylation from Liver Homogenates of Zucker Rats.

Histone 4 Lys 12 was analyzed by Western blot analysis as described in Materials and Methods 50 μ g of liver Protein Samples was separated by 12% SDS-PAGE gel and transferred onto PVDF membranes. The membrane was cut and probed with primary anti-histone 4 Lys 12 and β -actin separately at a final dilution of 1:5000 and 1:10000 respectively. Then secondary antibody (a goat anti-rabbit HRP conjugated) and (a goat anti-mouse HRP conjugated) at a final dilution of 1:5000 and 1:10000 for histone and β -actin was used respectively. The blots were exposed by ECL Plus substrate and developed on X-Ray film. Representative western blots of H4 Lys 12 and β -actin using 50 μ g of liver protein from Zucker Obese (Ob) and Lean (Ln) rats.

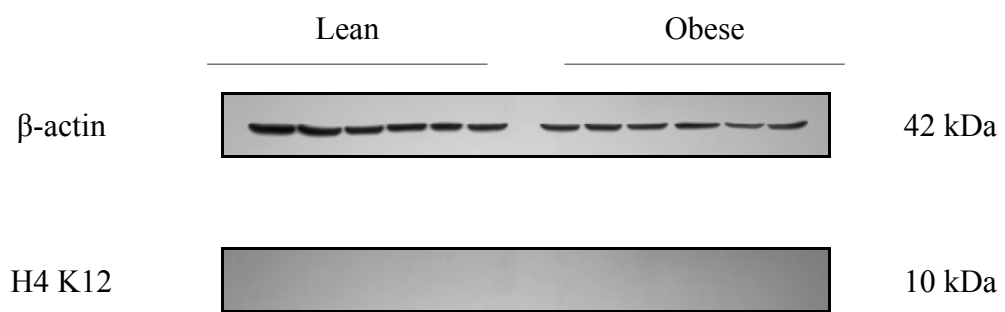


Figure 13: Summary of normalized densitometry quantification of histone acetylation from Liver Homogenates of Zucker Rats.

(a) Histone 3 (Lys 9) Histone Acetylation from Liver Homogenates of Zucker Rats. (b) Histone 3 (Lys 14) Histone Acetylation from Liver Homogenates of Zucker Rats. (c) Histone 4 (Lys 5) Histone Acetylation from Liver Homogenates of Zucker Rats.

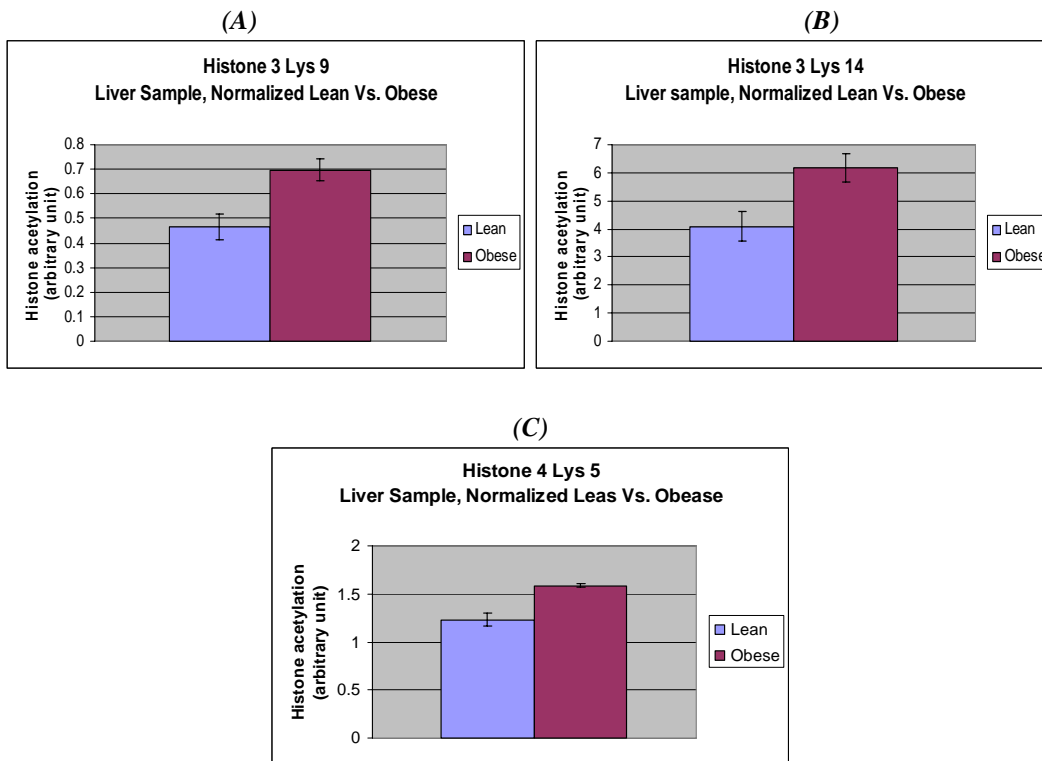
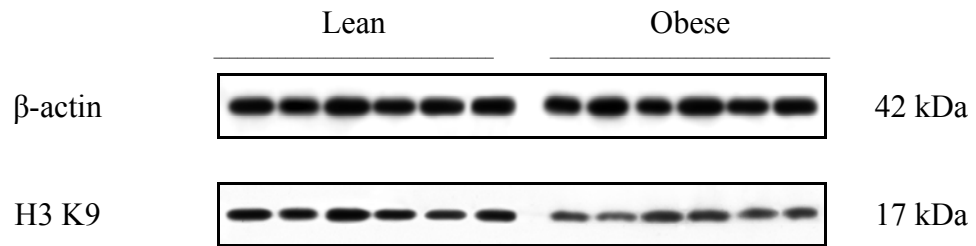


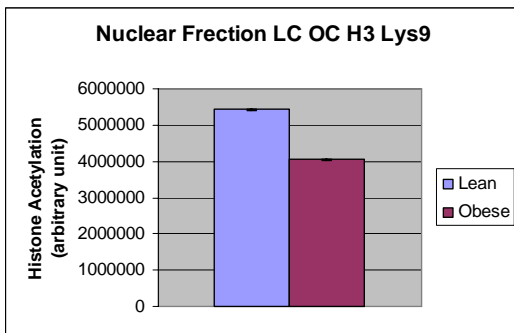
Figure 14: Western Blot Analysis of Histone 3 (Lys 9) Histone Acetylation from Liver Nuclear Fraction of Zucker Rats.

Histone 3 Lys 9 was analyzed by Western blot analysis as described in Materials and Methods 50 μ g of liver Protein Samples was separated by 12% SDS-PAGE gel and transferred onto PVDF membranes. The membrane was cut and probed with primary anti-histone 3 Lys 9 and β -actin separately at a final dilution of 1:7500 and 1:2500 respectively. Then secondary antibody (a goat anti-rabbit HRP conjugated) and (a goat anti-mouse HRP conjugated) at a final dilution of 1:5000 and 1:2500 for histone and β -actin was used respectively. The blots were exposed by ECL Plus substrate and developed on X-Ray film. (A) Representative western blots of H3 Lys 9 and β -actin using 50 μ g of liver protein from Zucker Obese (Ob) and Lean (Ln) rats. (B) shows densitometric quantitation $p < 0.05$ as determined by Independent-Samples T-test. Bar graph represents level of H3 Lys 9 protein of the relative intensities of H3 Lys 9 bands. The standard deviations of the experiment for each group of 6 animals are shown on the bars as determined by descriptive analysis. (C) shows normalized densitometric quantitation $p < 0.05$ as determined by Independent-Samples T-test. Bar graph represents level of H3 Lys 9 protein of the relative intensities of H3 Lys 9 bands normalized to β -actin. The standard deviations of the experiment for each group of 6 animals are shown on the bars as determined by descriptive analysis.

(A)



(B)



(C)

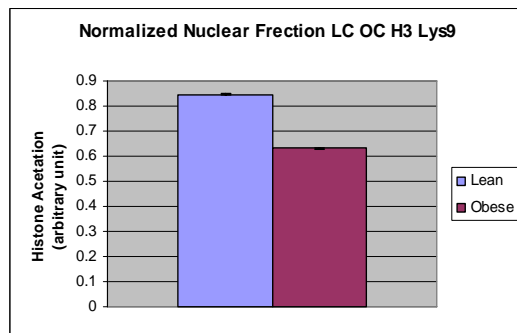
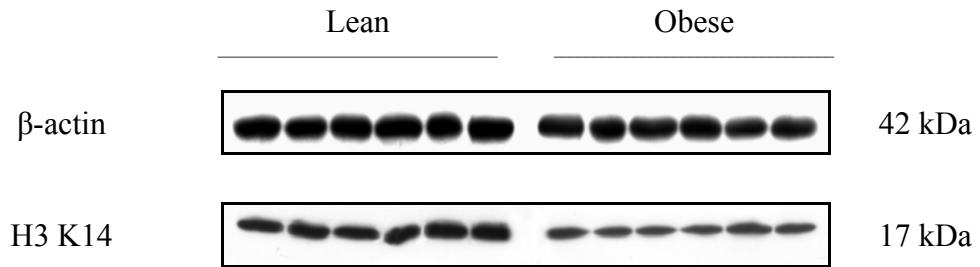


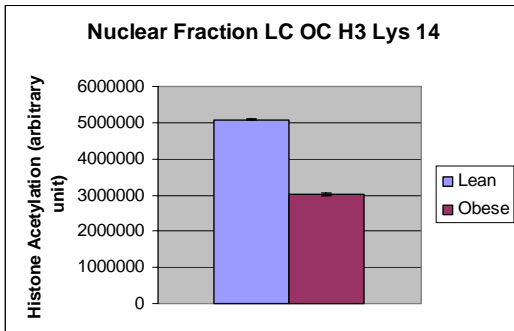
Figure 15: Western Blot Analysis of Histone 3 (Lys 14) Histone Acetylation from Liver Nuclear Fraction of Zucker Rats.

Histone 3 Lys14 was analyzed by Western blot analysis as described in Materials and Methods 50 µg of liver Protein Samples was separated by 12% SDS-PAGE gel and transferred onto PVDF membranes. The membrane was cut and probed with primary anti-histone 3 Lys 14 and β-actin separately at a final dilution of 1:2500 and 1:2500 respectively. Then secondary antibody (a goat anti-rabbit HRP conjugated) and (a goat anti-mouse HRP conjugated) at a final dilution of 1:5000 and 1:2500 for histone and β-actin was used respectively. The blots were exposed by ECL Plus substrate and developed on X-Ray film. (A) Representative western blots of H3 Lys 14 and β-actin using 50 µg of liver protein from Zucker Obese (Ob) and Lean (Ln) rats. (B) shows densitometric quantitation $p < 0.05$ as determined by Independent-Samples T-test. Bar graph represents level of H3 Lys 14 protein of the relative intensities of H3 Lys 14 bands. The standard deviations of the experiment for each group of 6 animals are shown on the bars as determined by descriptive analysis. (C) shows normalized densitometric quantitation $p < 0.05$ as determined by Independent-Samples T-test. Bar graph represents level of H3 Lys 14 protein of the relative intensities of H3 Lys 14 bands normalized to β-actin. The standard deviations of the experiment for each group of 6 animals are shown on the bars as determined by descriptive analysis.

(A)



(B)



(C)

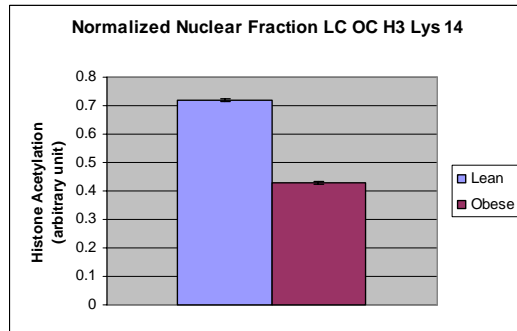
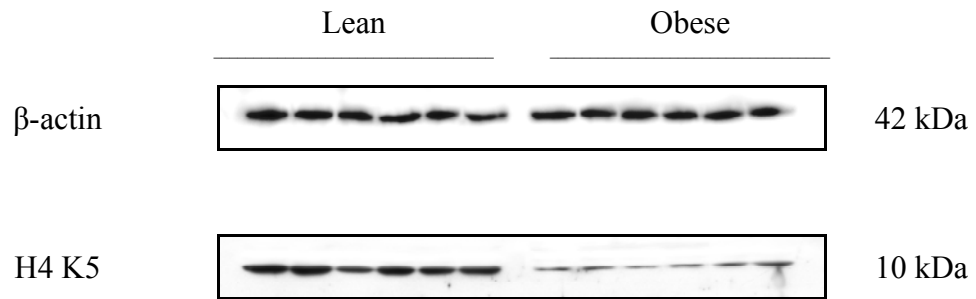


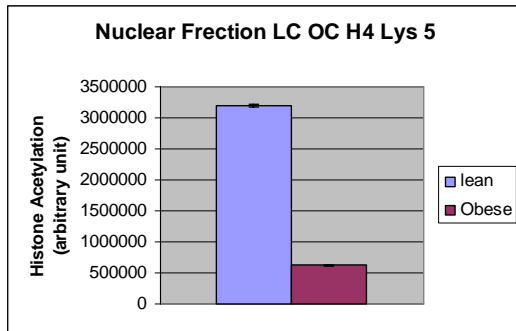
Figure 16: Western Blot Analysis of Histone 4 (Lys 5) Histone Acetylation from Liver Nuclear Fraction of Zucker Rats.

Histone 4 Lys 5 was analyzed by Western blot analysis as described in Materials and Methods 50 µg of liver Protein Samples was separated by 12% SDS-PAGE gel and transferred onto PVDF membranes. The membrane was cut and probed with primary anti-histone 4 Lys 5 and β-actin separately at a final dilution of 1:1000 and 1:10000 respectively. Then secondary antibody (a goat anti-rabbit HRP conjugated) and (a goat anti-mouse HRP conjugated) at a final dilution of 1:5000 and 1:10000 for histone and β-actin was used respectively. The blots were exposed by ECL Plus substrate and developed on X-Ray film. (A) Representative western blots of H4 Lys 5 and β-actin using 50 µg of liver protein from Zucker Obese (Ob) and Lean (Ln) rats. (B) shows densitometric quantitation $p < 0.05$ as determined by Independent-Samples T-test. Bar graph represents level of H4 Lys 5 protein of the relative intensities of H4 Lys 5 bands. The standard deviations of the experiment for each group of 6 animals are shown on the bars as determined by descriptive analysis. (C) shows normalized densitometric quantitation $p < 0.05$ as determined by Independent-Samples T-test. Bar graph represents level of H4 Lys 5 protein of the relative intensities of H4 Lys 5 bands normalized to β-actin. The standard deviations of the experiment for each group of 6 animals are shown on the bars as determined by descriptive analysis.

(A)



(B)



(C)

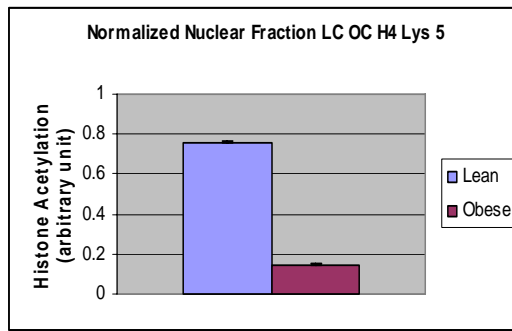


Figure 17: Western Blot Analysis of Histone 4 (Lys 12) Histone Acetylation from Liver Nuclear Fraction of Zucker Rats.

Histone 4 Lys 12 was analyzed by Western blot analysis as described in Materials and Methods 50 µg of liver Protein Samples was separated by 12% SDS-PAGE gel and transferred onto PVDF membranes. The membrane was cut and probed with primary anti-histone 4 Lys 12 and β-actin separately at a final dilution of 1:5000 and 1:5000 respectively. Then secondary antibody (a goat anti-rabbit HRP conjugated) and (a goat anti-mouse HRP conjugated) at a final dilution of 1:5000 and 1:5000 for histone and β-actin was used respectively. The blots were exposed by ECL Plus substrate and developed on X-Ray film. Representative western blots of H4 Lys 12 and β-actin using 50 µg of liver protein from Zucker Obese (Ob) and Lean (Ln) rats.

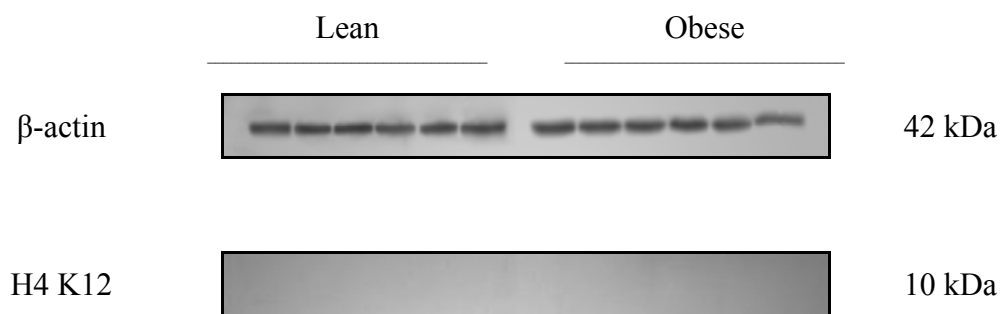
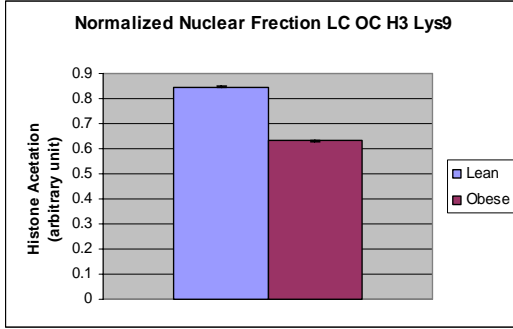


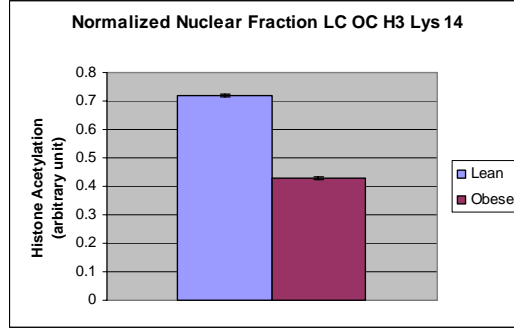
Figure 18: Summary of normalized densitometry quantification of Liver Nuclear Fractions in Zucker Rats.

(a) Histone 3 (Lys 9) Histone Acetylation from Liver Nuclear Fractions of Zucker Rats. (b) Histone 3 (Lys 14) Histone Acetylation from Liver Nuclear Fractions in Zucker Rats. (c) Histone 4 (Lys 5) Histone Acetylation from Liver nuclear fractions in Zucker Rats.

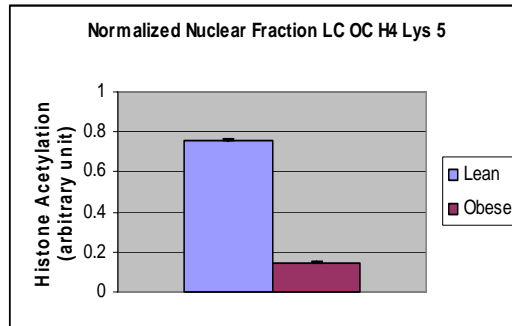
(A)



(B)



(C)



3.2 Protein Expression Pattern in Obese with High Vitamin B6 vs. Obese with Normal Vitamin B6 (OH/ON)

Western blots were performed to assess relative whole homogenate and nuclear extract protein levels of H3 and H4 acetylation at specific lysine residues. The level of vitamin B6 was increased five fold in the group of obese animals abbreviated as (OH) in compare with obese with normal vitamin B6 abbreviated as (ON).

3.2.1 Identification of Global as well as Specific Lysines Acetylated on Histone H3 and H4

The effect of vitamin B6 on histone acetylation is not yet known. From present study we know that the level of global acetylation of H3 and H4 slightly reduced in obese rats. We also obtained that nuclear acetylation of H3 and H4 decreases at specific lysine residues in the liver of obese rats in comparison with their lean counterparts. Furthermore, we know that high B6 diet reduces liver weight as well as the number of preneoplastic lesions in the Zucker obese rats (A. Kular study). These new results were suggestive to examine if a positive effect of vitamin B6 is associated with changes in the level and pattern of H3 and H4 acetylation. In order to address this question, we similarly examined the level and pattern of global acetylation as well as homogenate and nuclear acetylation at lysines (K9, K14, K5, K12) acetylated in livers of obese rats fed a normal amount of vitamin B6 (ON) and those fed five times higher amount of vitamin B6 (OH). If hyperacetylation could play a role as a protective response to hepatic steatosis then we expect to see enhancement of global acetylation of H3 and H4 as well as hyperacetylation in nuclear fractions of OH group. The levels of histone H3 and H4 acetylation slightly

enhanced in both liver homogenate and nuclear fractions in obese animals feeding high amount of vitamin B6 (summary is in figure 23). There was a slightly significant increase in the level of acetylation in homogenate and nuclear fractions of histone H3 at lysine K9, K14, and H4 at K5 (summary is in figure 28 & 33). We were not able to detect acetylation of K12 in histone H4 for either homogenate or nuclear fractions (Figure 27 and 32 respectively). From these observations, it appears possible that hyperacetylation may possibly participate in amelioration of hepatic steatosis. One possibility can be explained by antioxidant affect of B6 which reduce the level of oxidative stress markers which in turn can affect acetylation levels.

3.3 Identification of the level of Bax and Bcl-2 protein expression in LC/OC and OH/ON group

It is known that obese rat contains more oxidative stress as the result of respiration and glucose metabolism. On the other hand, oxidative stress and inflammatory mediators activate transcription factors leading to the expression of pro-inflammatory genes which in turn involves the remodeling of the chromatin structure by the histone protein [72].

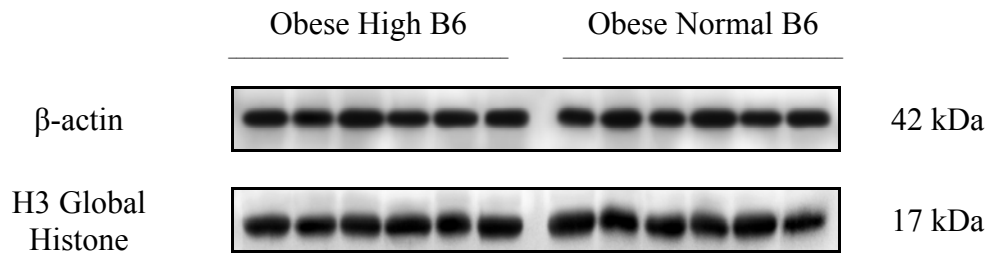
It is also known that oxidative stress can trigger apoptotic pathway. Therefore, anti- and pro-apoptotic Bax and Bcl-2 expression in obese versus lean and obese fed high amount of vitamin B6 versus obese fed normal amount of vitamin B6 by western blot were effectively examined. Quantification of the band densities after normalization with beta actin shows that obese animals have higher level of Bax but lower level of anti-apoptotic Bcl-2, in compare to the lean counterparts, as expected (figure 34 and 35). In OH versus ON, unexpectedly, obese with healthier liver (OH) had higher amount of Bax and lower

amount of Bcl-2 (figure 36 and 37). An extensive discussion on this topic is presented later (summary is in figure 38).

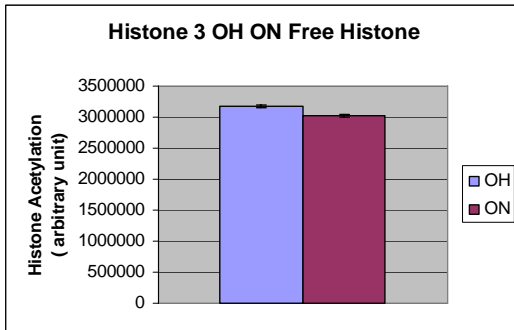
Figure 19: Western Blot Analysis of Histone 3 (Global Histone 3) Histone Acetylation From Liver Homogenates of Zucker Obese Rats.

Histone 3 (H3) was analyzed by Western blot analysis as described in Materials and Methods 50 µg of liver Protein Samples was separated by 12% SDS-PAGE gel and transferred onto PVDF membranes. The membrane was cut and probed with primary anti-histone 3 and β-actin separately at a final dilution of 1:500 and 1:5000 respectively. Then secondary antibody (a goat anti-rabbit HRP conjugated) and (a goat anti-mouse HRP conjugated) at a final dilution of 1:5000 and 1:5000 for histone and β-actin was used respectively. The blots were exposed by ECL Plus substrate and developed on X-Ray film. (A) Representative western blots of H3 and β-actin using 50 µg of liver protein from Zucker Obese with high vitamin B6 (OH) and Zucker Obese with normal vitamin B6 (ON). (B) shows densitometric quantitation $p < 0.05$ as determined by Independent-Samples T-test. Bar graph represents level of H3 protein of the relative intensities of H3 bands. The standard deviations of the experiment for each group of 6 animals are shown on the bars as determined by descriptive analysis. (C) shows normalized densitometric quantitation $p < 0.05$ as determined by Independent-Samples T-test. Bar graph represents level of H3 protein of the relative intensities of H3 bands normalized to β-actin. The standard deviations of the experiment for each group of 6 animals are shown on the bars as determined by descriptive analysis.

(A)



(B)



(C)

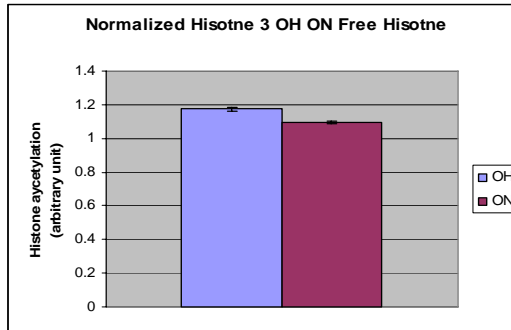


Figure 20: Western Blot Analysis of Histone 4 (Global Histone 4) Histone Acetylation From Liver Homogenates of Zucker Obese Rats.

Histone 4 (H4) was analyzed by Western blot analysis as described in Materials and Methods 50 µg of liver Protein Samples was separated by 12% SDS-PAGE gel and transferred onto PVDF membranes. The membrane was cut and probed with primary anti-histone 4 and β-actin separately at a final dilution of 1:500 and 1:5000 respectively. Then secondary antibody (a goat anti-rabbit HRP conjugated) and (a goat anti-mouse HRP conjugated) at a final dilution of 1:5000 and 1:5000 for histone and β-actin was used respectively. The blots were exposed by ECL Plus substrate and developed on X-Ray film. (A) Representative western blots of H4 and β-actin using 50 µg of liver protein from Zucker Obese with high vitamin B6 (OH) and Zucker Obese with normal vitamine B6 (ON). (B) shows ensitometric quantitation $p < 0.05$ as determined by Independent-Samples T-test. Bar graph represents level of H4 protein of the relative intensities of H4 bands. The standard deviations of the experiment for each group of 6 animals are shown on the bars as determined by descriptive analysis. (C) shows normalized densitometric quantitation $p < 0.05$ as determined by Independent-Samples T-test. Bar graph represents level of H4 protein of the relative intensities of H4 bands normalized to β-actin. The standard deviations of the experiment for each group of 6 animals are shown on the bars as determined by descriptive analysis.

(A)

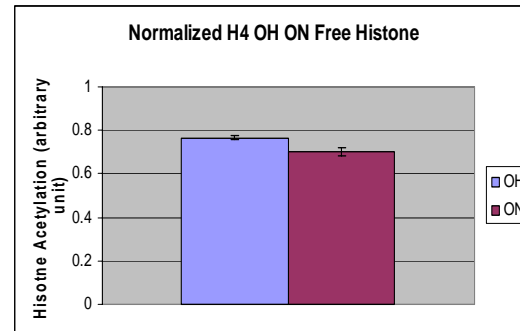
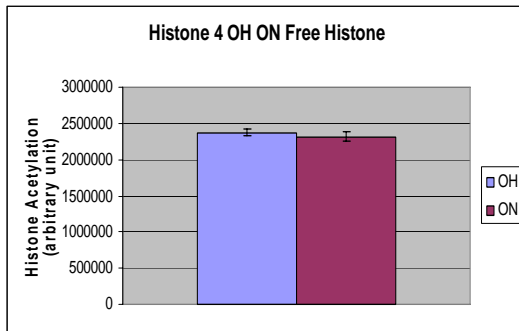
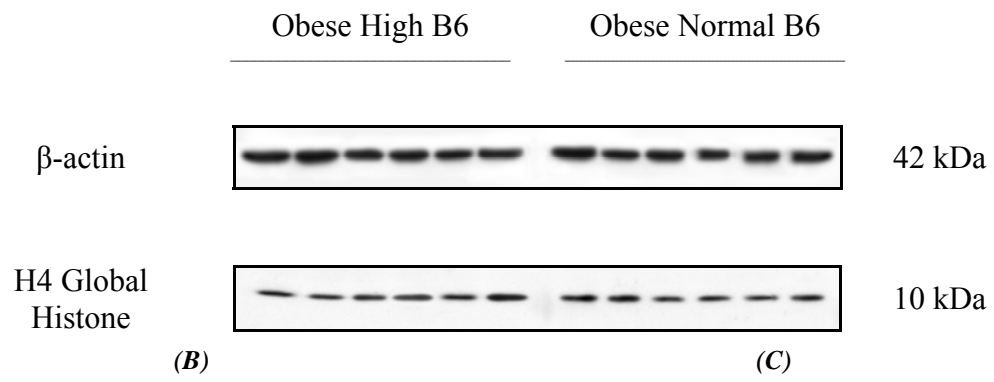
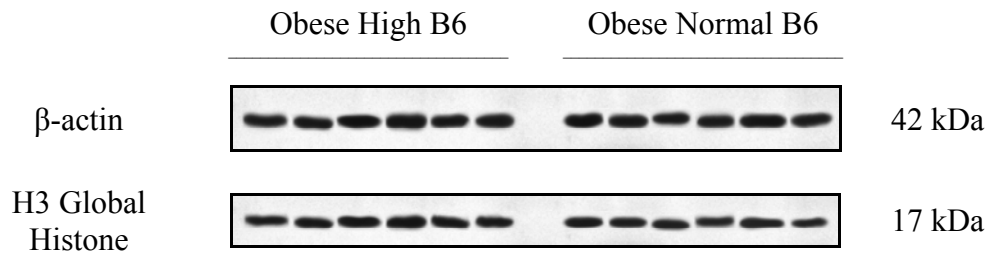


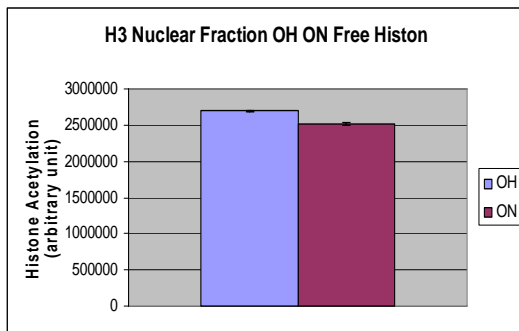
Figure 21: Western Blot Analysis of Histone 3 (Global Histone) Histone Acetylation From Liver Nuclear Fractions of Zucker Obese Rats.

Histone 3 (H3) was analyzed by Western blot analysis as described in Materials and Methods 50 µg of liver Protein Samples was separated by 12% SDS-PAGE gel and transferred onto PVDF membranes. The membrane was cut and probed with primary anti-histone 3 and β-actin separately at a final dilution of 1:500 and 1:5000 respectively. Then secondary antibody (a goat anti-rabbit HRP conjugated) and (a goat anti-mouse HRP conjugated) at a final dilution of 1:5000 and 1:5000 for histone and β-actin was used respectively. The blots were exposed by ECL Plus substrate and developed on X-Ray film. (A) Representative western blots of H3 and β-actin using 50 µg of liver protein from Zucker Obese with high vitamin B6 (OH) and Zucker Obese with normal vitamin B6 (ON). (B) shows densitometric quantitation $p < 0.05$ as determined by Independent-Samples T-test. Bar graph represents level of H3 protein of the relative intensities of H3 bands. The standard deviations of the experiment for each group of 6 animals are shown on the bars as determined by descriptive analysis. (C) shows normalized densitometric quantitation $p < 0.05$ as determined by Independent-Samples T-test. Bar graph represents level of H3 protein of the relative intensities of H3 bands normalized to β-actin. The standard deviations of the experiment for each group of 6 animals are shown on the bars as determined by descriptive analysis.

(A)



(B)



(C)

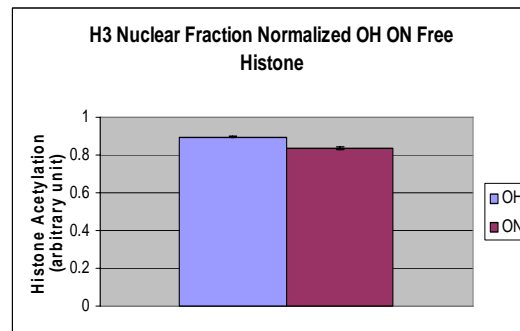


Figure 22: Western Blot Analysis of Histone 4 (Global Histone) Histone Acetylation From Liver Nuclear Fractions of Zucker Obese Rats.

Histone 4 (H4) was analyzed by Western blot analysis as described in Materials and Methods 50 µg of liver Protein Samples was separated by 12% SDS-PAGE gel and transferred onto PVDF membranes. The membrane was cut and probed with primary anti-histone 4 and β-actin separately at a final dilution of 1:500 and 1:5000 respectively. Then secondary antibody (a goat anti-rabbit HRP conjugated) and (a goat anti-mouse HRP conjugated) at a final dilution of 1:5000 and 1:5000 for histone and β-actin was used respectively. The blots were exposed by ECL Plus substrate and developed on X-Ray film. (A) Representative western blots of H4 and β-actin using 50 µg of liver protein from Zucker Obese with high vitamin B6 (OH) and Zucker Obese with normal vitamine B6 (ON). (B) shows ensitometric quantitation $p < 0.05$ as determined by Independent-Samples T-test. Bar graph represents level of H4 protein of the relative intensities of H4 bands. The standard deviations of the experiment for each group of 6 animals are shown on the bars as determined by descriptive analysis. (C) shows normalized densitometric quantitation $p < 0.05$ as determined by Independent-Samples T-test. Bar graph represents level of H4 protein of the relative intensities of H4 bands normalized to β-actin. The standard deviations of the experiment for each group of 6 animals are shown on the bars as determined by descriptive analysis.

(A)

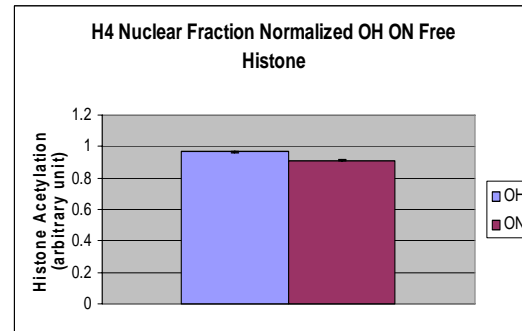
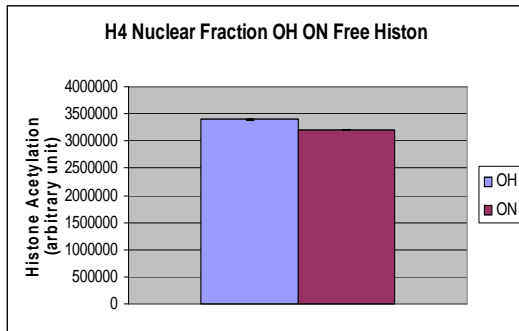
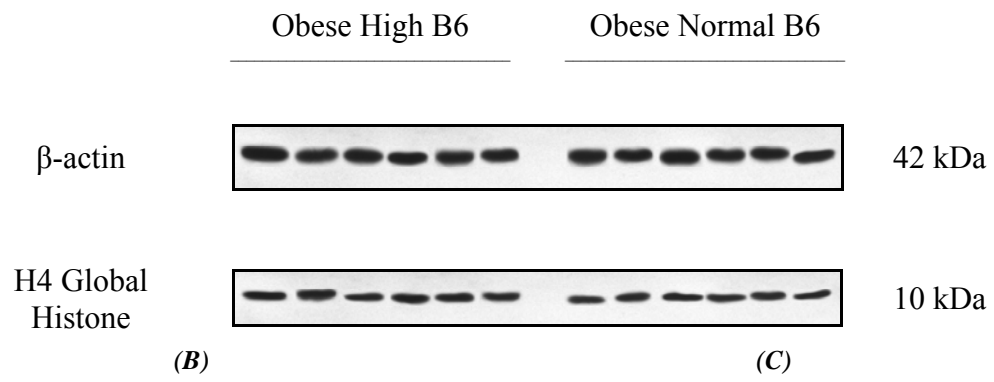
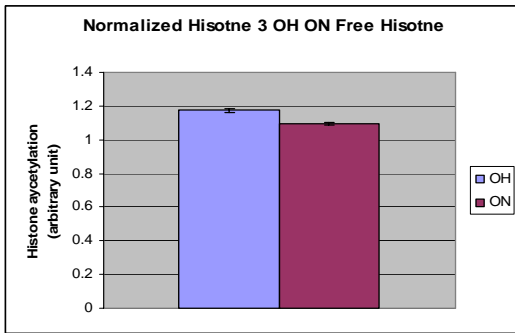


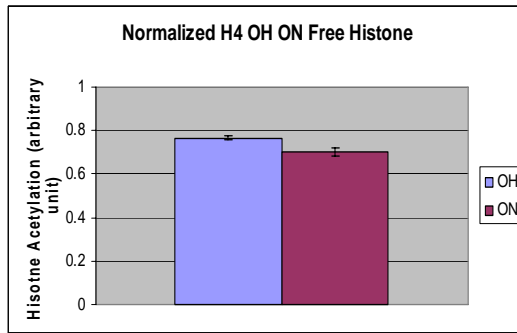
Figure 23: Summary of normalized densitometry quantification of Histone Acetylation From Liver Homogenates of Zucker Obese Rats.

(a) Histone 3 (Global Histone) histone acetylation from liver homogenates of Zucker obese rats. (b) Histone 4 (Global Histone) histone acetylation from liver homogenates of Zucker obese rats. (c) Histone 3 (Global Histone) histone acetylation from liver nuclear fractions of Zucker obese rats. (d) Histone 4 (Global Histone) histone acetylation from liver nuclear fractions of Obese Zucker Rats.

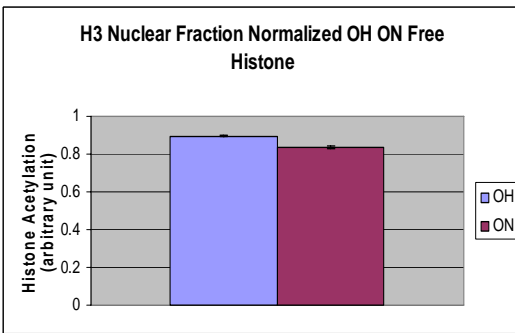
(A)



(B)



(C)



(D)

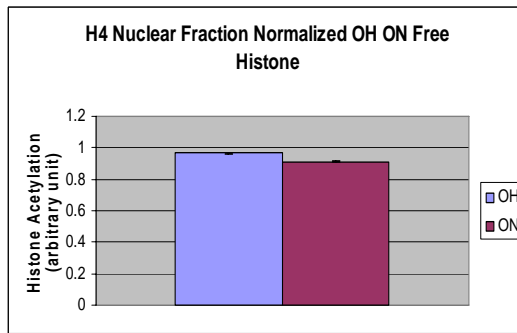
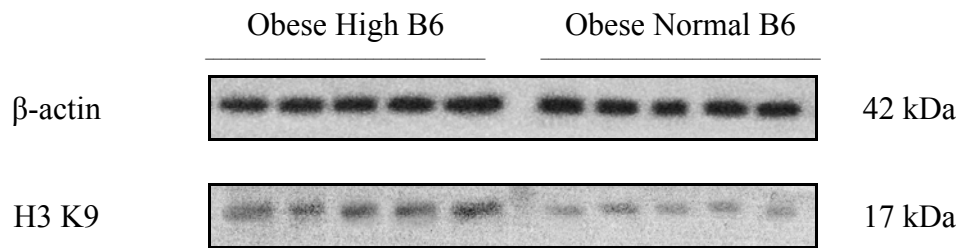


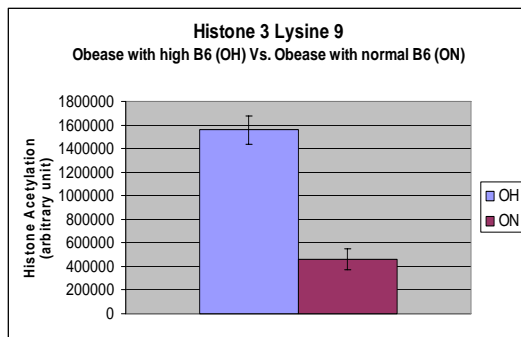
Figure 24: Western Blot Analysis of Histone 3 (Lys 9) Histone Acetylation from Liver Homogenates of Zucker Obese Rats.

Histone 3 Lys 9 was analyzed by Western blot analysis as described in Materials and Methods 50 μ g of liver Protein Samples was separated by 12% SDS-PAGE gel and transferred onto PVDF membranes. The membrane was cut and probed with primary anti-histone 3 Lys 9 and β -actin separately at a final dilution of 1:7500 and 1:5000 respectively. Then secondary antibody (a goat anti-rabbit HRP conjugated) and (a goat anti-mouse HRP conjugated) at a final dilution of 1:5000 and 1:5000 for histone and β -actin was used respectively. The blots were exposed by ECL Plus substrate and developed on X-Ray film. (A) Representative western blots of H3 Lys 9 and β -actin using 50 μ g of liver protein from Zucker Obese with high vitamin B6 (OH) and Zucker Obese with normal vitamin B6 (ON). (B) shows densitometric quantitation $p < 0.05$ as determined by Independent-Samples T-test. Bar graph represents level of H3 Lys 9 protein of the relative intensities of H3 Lys 9 bands. The standard deviations of the experiment for each group of 6 animals are shown on the bars as determined by descriptive analysis. (C) shows normalized densitometric quantitation $p < 0.05$ as determined by Independent-Samples T-test. Bar graph represents level of H3 Lys 9 protein of the relative intensities of H3 Lys 9 bands normalized to β -actin. The standard deviations of the experiment for each group of 6 animals are shown on the bars as determined by descriptive analysis.

(A)



(B)



(C)

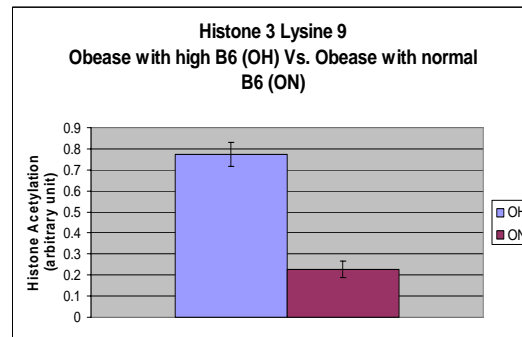
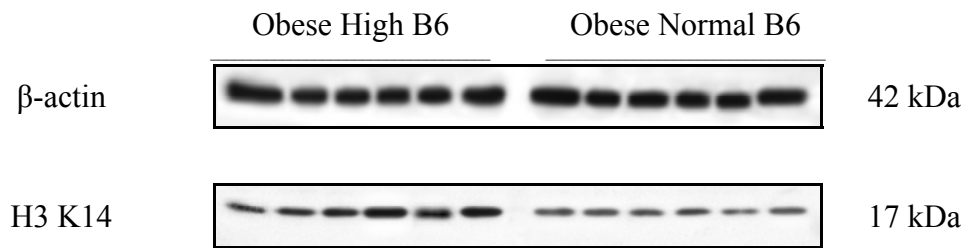


Figure 25: Western Blot Analysis of Histone 3 (Lys 14) Histone Acetylation from Liver Homogenates of Zucker Obese Rats.

Histone 3 Lys14 was analyzed by Western blot analysis as described in Materials and Methods 50 μ g of liver Protein Samples was separated by 12% SDS-PAGE gel and transferred onto PVDF membranes. The membrane was cut and probed with primary anti-histone 3 Lys 14 and β -actin separately at a final dilution of 1:2500 and 1:25000 respectively. Then secondary antibody (a goat anti-rabbit HRP conjugated) and (a goat anti-mouse HRP conjugated) at a final dilution of 1:5000 and 1:2500 for histone and β -actin was used respectively. The blots were exposed by ECL Plus substrate and developed on X-Ray film. (A) Representative western blots of H3 Lys 14 and β -actin using 50 μ g of liver protein from Zucker Obese with high vitamin B6 (OH) and Zucker Obese with normal vitamine B6 (ON). (B) shows densitometric quantitation $p < 0.05$ as determined by Independent-Samples T-test. Bar graph represents level of H3 Lys 14 protein of the relative intensities of H3 Lys 14 bands. The standard deviations of the experiment for each group of 6 animals are shown on the bars as determined by descriptive analysis. (C) shows normalized densitometric quantitation $p < 0.05$ as determined by Independent-Samples T-test. Bar graph represents level of H3 Lys 14 protein of the relative intensities of H3 Lys 14 bands normalized to β -actin. The standard deviations of the experiment for each group of 6 animals are shown on the bars as determined by descriptive analysis.

(A)



(B)



(C)

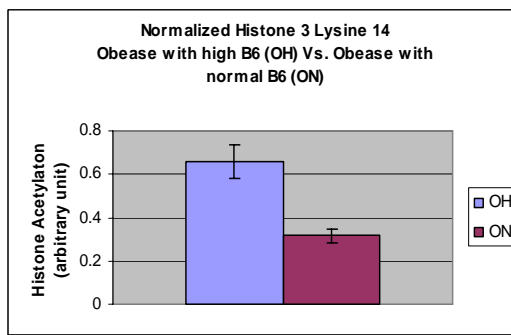
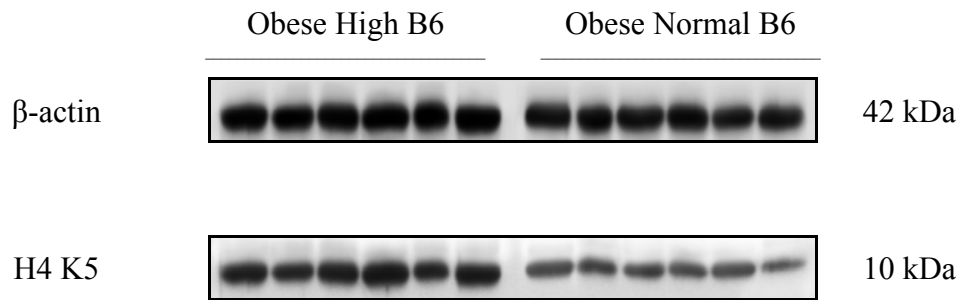


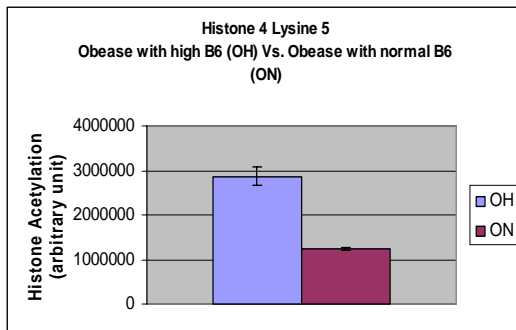
Figure 26: Western Blot Analysis of Histone 4 (Lys 5) Histone Acetylation from Liver Homogenates of Zucker Obese Rats.

Histone 4 Lys 5 was analyzed by Western blot analysis as described in Materials and Methods. The membrane from figure 19 was washed and reprobed with primary anti-histone 4 Lys 5 and β -actin separately at a final dilution of 1:1000 and 1:2500 respectively. Then secondary antibody (a goat anti-rabbit HRP conjugated) and (a goat anti-mouse HRP conjugated) at a final dilution of 1:5000 and 1:2500 for histone and β -actin was used respectively. The blots were exposed by ECL Plus substrate and developed on X-Ray film. (A) Representative western blots of H4 Lys 5 and β -actin using 50 μ g of liver protein from Zucker Obese with high vitamin B6 (OH) and Zucker Obese with normal vitamin B6 (ON). (B) shows densitometric quantitation $p < 0.05$ as determined by Independent-Samples T-test. Bar graph represents level of H4 Lys 5 protein of the relative intensities of H4 Lys 5 bands. The standard deviations of the experiment for each group of 6 animals are shown on the bars as determined by descriptive analysis. (C) shows normalized densitometric quantitation $p < 0.05$ as determined by Independent-Samples T-test. Bar graph represents level of H4 Lys 5 protein of the relative intensities of H4 Lys 5 bands normalized to β -actin. The standard deviations of the experiment for each group of 6 animals are shown on the bars as determined by descriptive analysis.

(A)



(B)



(C)

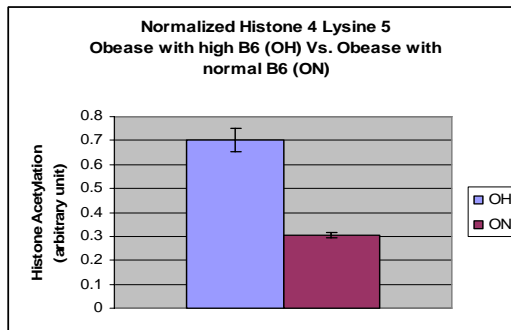


Figure 27: Western Blot Analysis of Histone 3 (Lys 12) Histone Acetylation from Liver Homogenates of Zucker Obese Rats.

Histone 4 Lys 12 was analyzed by Western blot analysis as described in Materials and Methods 50 µg of liver Protein Samples was separated by 12% SDS-PAGE gel and transferred onto PVDF membranes. The membrane was cut and probed with primary anti-histone 4 Lys 12 and β-actin separately at a final dilution of 1:5000 and 1:5000 respectively. Then secondary antibody (a goat anti-rabbit HRP conjugated) and (a goat anti-mouse HRP conjugated) at a final dilution of 1:5000 and 1:20000 for histone and β-actin was used respectively. The blots were exposed by ECL Plus substrate and developed on X-Ray film. Representative western blots of H4 Lys 12 and β-actin using 50 µg of liver protein from Zucker Obese with high vitamin B6 (OH) and Zucker Obese with normal vitamin B6 (ON).

(A)

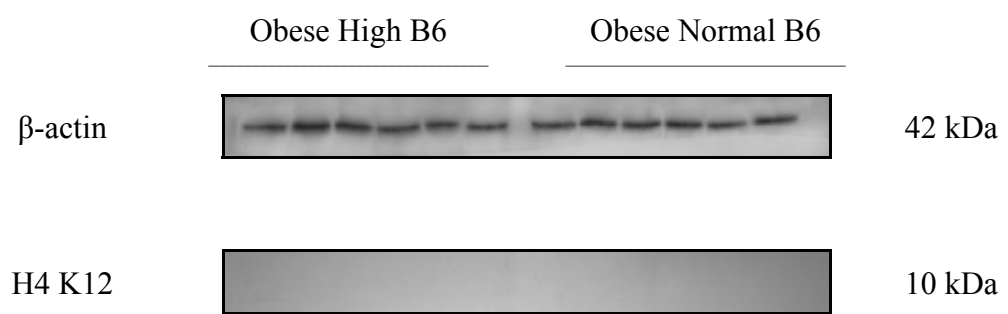
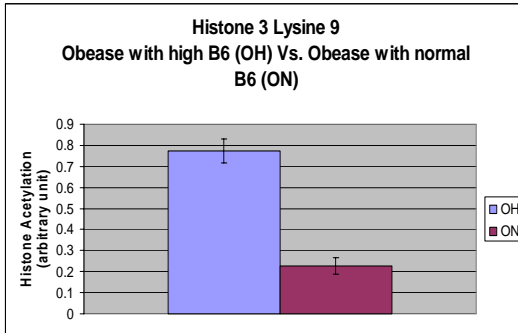


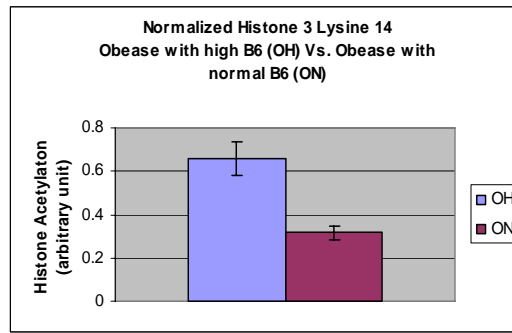
Figure 28: Summary of normalized densitometry quantification of histone acetylation from Liver Homogenates of Zucker Obese Rats.

(a) Histone 3 (Lys 9) histone acetylation from Liver Homogenates of Obese Zucker Rats. (b) Histone 3 (Lys 9) histone acetylation from Liver Homogenates of Obese Zucker Rats. (c) Histone 4 (Lys 5) histone acetylation from Liver Homogenates of Obese Zucker Rats.

(A)



(B)



(C)

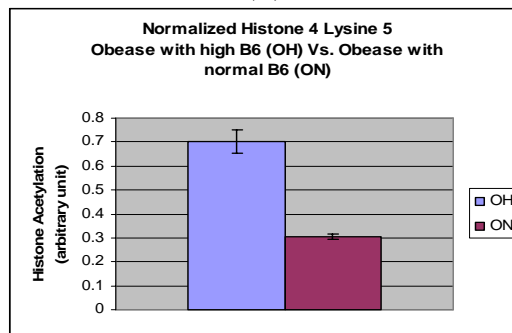
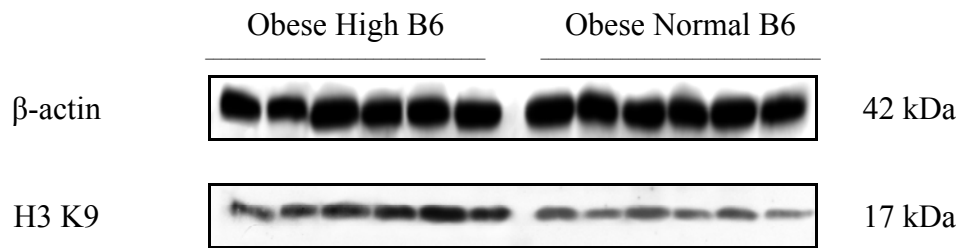


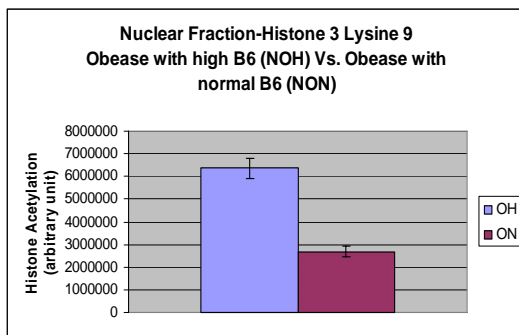
Figure 29: Western Blot Analysis of Histone 3 (Lys 9) Histone Acetylation from Liver Nuclear Fraction of Zucker Obese Rats.

Histone 3 Lys 9 was analyzed by Western blot analysis as described in Materials and Methods 50 μ g of liver Protein Samples was separated by 12% SDS-PAGE gel and transferred onto PVDF membranes. The membrane was cut and probed with primary anti-histone 3 Lys 9 and β -actin separately at a final dilution of 1:7500 and 1:2500 respectively. Then secondary antibody (a goat anti-rabbit HRP conjugated) and (a goat anti-mouse HRP conjugated) at a final dilution of 1:5000 and 1:2500 for histone and β -actin was used respectively.. The blots were exposed by ECL Plus substrate and developed on X-Ray film. (A) Representative western blots of H3 Lys 9 and β -actin using 50 μ g of liver protein from Zucker Obese with high vitamin B6 (OH) and Zucker Obese with normal vitamine B6 (ON). (B) shows densitometric quantitation $p < 0.05$ as determined by Independent-Samples T-test. Bar graph represents level of H3 Lys 9 protein of the relative intensities of H3 Lys 9 bands. The standard deviations of the experiment for each group of 6 animals are shown on the bars as determined by descriptive analysis. (C) shows normalized densitometric quantitation $p < 0.05$ as determined by Independent-Samples T-test. Bar graph represents level of H3 Lys 9 protein of the relative intensities of H3 Lys 9 bands normalized to β -actin. The standard deviations of the experiment for each group of 6 animals are shown on the bars as determined by descriptive analysis.

(A)



(B)



(C)

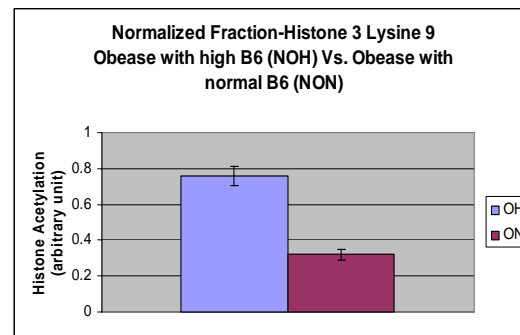
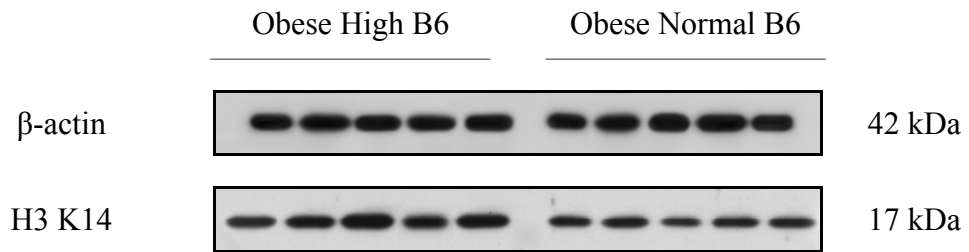


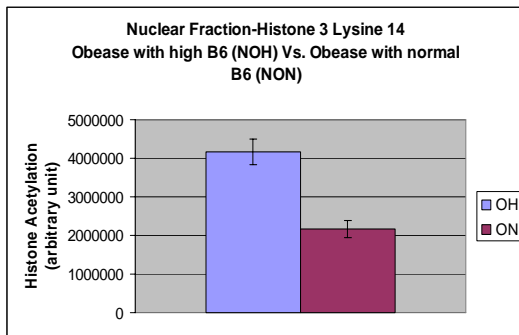
Figure 30: Western Blot Analysis of Histone 3 (Lys 14) Histone Acetylation from Liver Nuclear Fraction of Zucker Obese Rats.

Histone 3 Lys14 was analyzed by Western blot analysis as described in Materials and Methods 50 µg of liver Protein Samples was separated by 12% SDS-PAGE gel and transferred onto PVDF membranes. The membrane was cut and probed with primary anti-histone 3 Lys 14 and β-actin separately at a final dilution of 1:2500 and 1:5000 respectively. Then secondary antibody (a goat anti-rabbit HRP conjugated) and (a goat anti-mouse HRP conjugated) at a final dilution of 1:5000 and 1:5000 for histone and β-actin was used respectively. The blots were exposed by ECL Plus substrate and developed on X-Ray film. (A) Representative western blots of H3 Lys 14 and β-actin using 50 µg of liver protein from Zucker Obese with high vitamin B6 (OH) and Zucker Obese with normal vitamin B6 (ON). (B) shows densitometric quantitation $p < 0.05$ as determined by Independent-Samples T-test. Bar graph represents level of H3 Lys 14 protein of the relative intensities of H3 Lys 14 bands. The standard deviations of the experiment for each group of 6 animals are shown on the bars as determined by descriptive analysis. (C) shows normalized densitometric quantitation $p < 0.05$ as determined by Independent-Samples T-test. Bar graph represents level of H3 Lys 14 protein of the relative intensities of H3 Lys 14 bands normalized to β-actin. The standard deviations of the experiment for each group of 6 animals are shown on the bars as determined by descriptive analysis.

(A)



(B)



(C)

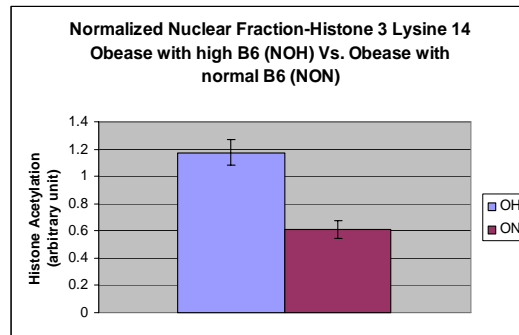
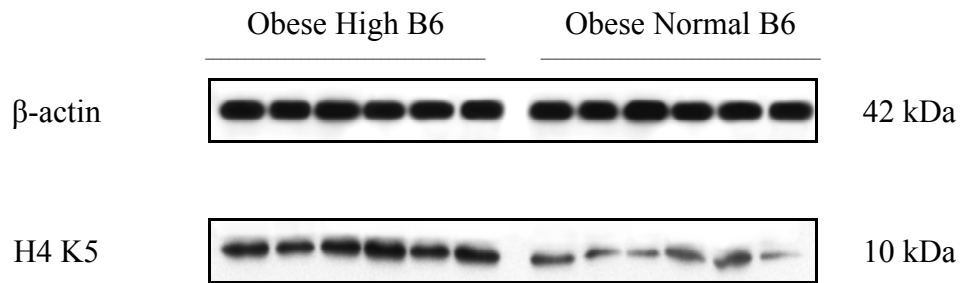


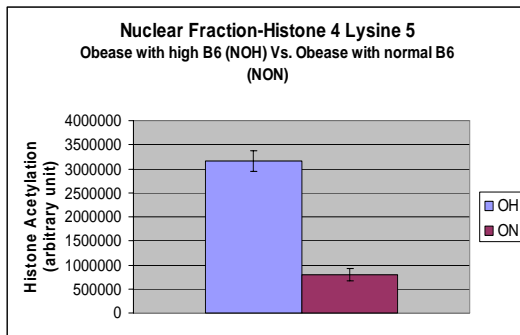
Figure 31: Western Blot Analysis of Histone 4 (Lys 5) Histone Acetylation from Liver Nuclear Fraction of Zucker Obese Rats.

Histone 4 Lys 5 was analyzed by Western blot analysis as described in Materials and Methods 50 µg of liver Protein Samples was separated by 12% SDS-PAGE gel and transferred onto PVDF membranes. The membrane was cut and probed with primary anti-histone 4 Lys 5 and 1:5000 respectively. at a final dilution of 1:1000 and 1:5000 respectively. Then secondary antibody (a goat anti-rabbit HRP conjugated) and (a goat anti-mouse HRP conjugated) at a final dilution of 1:5000 and 1:5000 for histone and β-actin was used respectively. The blots were exposed by ECL Plus substrate and developed on X-Ray film. (A) Representative western blots of H4 Lys 5 and β-actin using 50 µg of liver protein from Zucker Obese with high vitamin B6 (OH) and Zucker Obese with normal vitamin B6 (ON). (B) shows densitometric quantitation $p < 0.05$ as determined by Independent-Samples T-test. Bar graph represents level of H4 Lys 5 protein of the relative intensities of H4 Lys 5 bands. The standard deviations of the experiment for each group of 6 animals are shown on the bars as determined by descriptive analysis. (C) shows normalized densitometric quantitation $p < 0.05$ as determined by Independent-Samples T-test. Bar graph represents level of H4 Lys 5 protein of the relative intensities of H4 Lys 5 bands normalized to β-actin. The standard deviations of the experiment for each group of 6 animals are shown on the bars as determined by descriptive analysis.

(A)



(B)



(C)

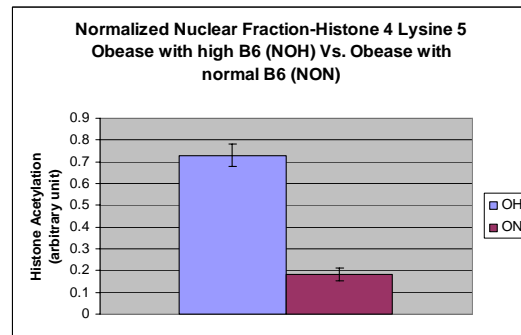


Figure 32: Western Blot Analysis of Histone 4 (Lys 12) Histone Acetylation from Liver Nuclear Fraction of Zucker Obese Rats.

Histone 4 Lys 12 was analyzed by Western blot analysis as described in Materials and Methods 50 µg of liver Protein Samples was separated by 12% SDS-PAGE gel and transferred onto PVDF membranes. The membrane was cut and probed with primary anti-histone 4 Lys 12 and β-actin separately at a final dilution of 1:5000 and 1:10000 respectively. Then secondary antibody (a goat anti-rabbit HRP conjugated) and (a goat anti-mouse HRP conjugated) at a final dilution of 1:5000 and 1:10000 for histone and β-actin was used respectively. The blots were exposed by ECL Plus substrate and developed on X-Ray film. Representative western blots of H4 Lys 12 and β-actin using 50 µg of liver protein from Zucker Obese with high vitamin B6 (OH) and Zucker Obese with normal vitamin B6 (ON).

(A)

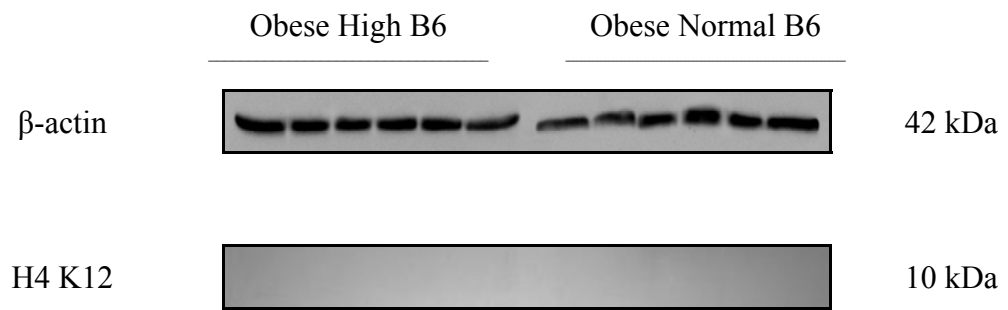
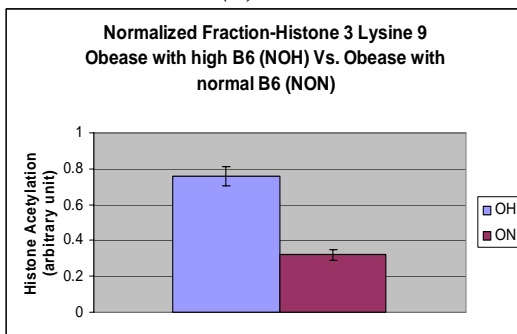


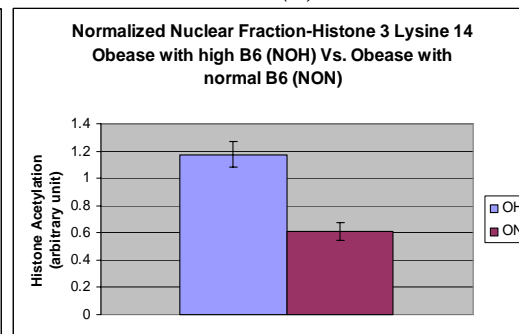
Figure 33: Summary of normalized densitometry quantification of Histone Acetylation from Liver Nuclear Fraction of Zucker Obese Rats.

(a) Histone 3 (Lys 9) Histone Acetylation from Liver Nuclear Fraction of Zucker Obese Rats. (b) Histone 3 (Lys 14) Histone Acetylation from Liver Nuclear Fraction of Zucker Obese Rats. Histone 4 (Lys 5) Histone Acetylation from Liver Nuclear Fraction of Zucker Obese Rats.

(A)



(B)



(C)

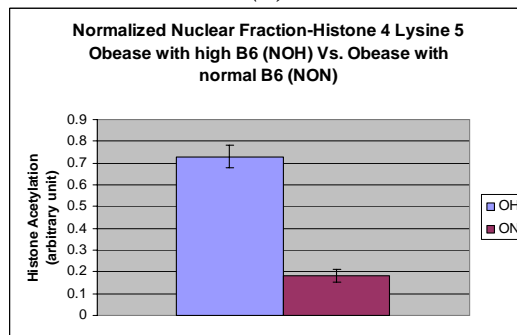
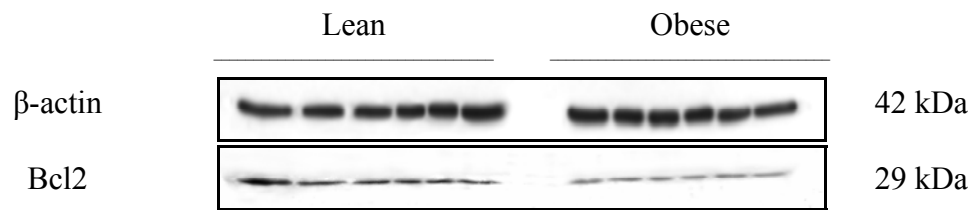


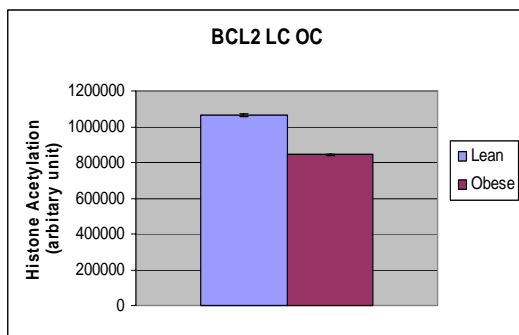
Figure 34: Western Blot Analysis of anti-apoptotic Bcl2 Protein expression from Liver Homogenates of Zucker Obese Rats.

Bcl2 was analyzed by Western blot analysis as described in Materials and Methods. 50 µg of liver Protein Samples was separated by 12% SDS-PAGE gel and transferred onto PVDF membranes. The blots were blocked about 4-5 hours. The membrane was probed with primary anti-Bcl2 and β-actin separately at a final dilution of 1:1000 and 1:5000 respectively. Then secondary antibody (a goat anti-rabbit HRP conjugated) and (a goat anti-mouse HRP conjugated) at a final dilution of 1:2500 and 1:5000 for histone and β-actin was used respectively. The blots were exposed by ECL Plus substrate and developed on X-Ray film. (A) Representative western blots of Bcl2 and β-actin using 50 µg of liver protein from Zucker Obese (Ob) and Lean (Ln) rats. (B) shows densitometric quantitation $p < 0.05$ as determined by Independent-Samples T-test. Bar graph represents level of Bcl2 protein of the relative intensities of Bcl2 bands. The standard deviations of the experiment for each group of 6 animals are shown on the bars as determined by descriptive analysis. (C) shows normalized densitometric quantitation $p < 0.05$ as determined by Independent-Samples T-test. Bar graph represents level of Bcl2 protein of the relative intensities of Bcl2 bands normalized to β-actin. The standard deviations of the experiment for each group of 6 animals are shown on the bars as determined by descriptive analysis.

(A)



(B)



(C)

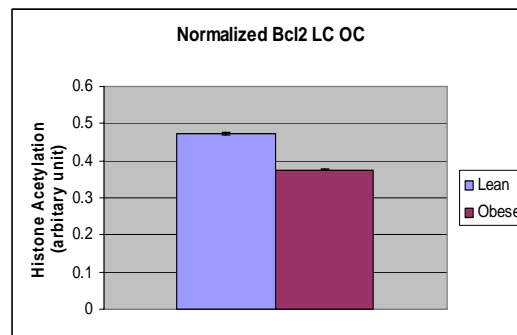
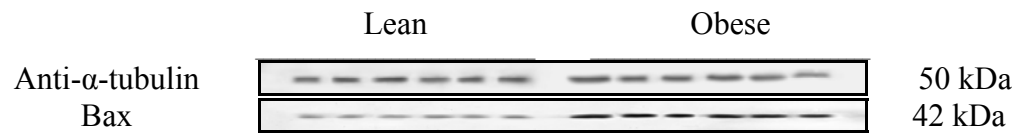


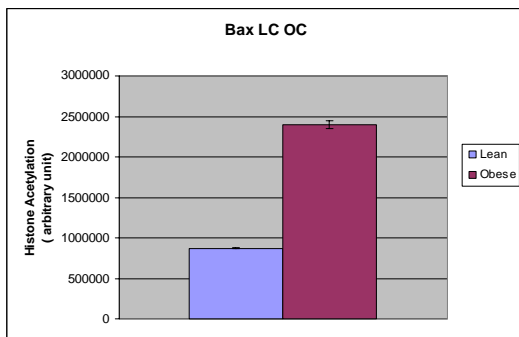
Figure 35: Western Blot Analysis of Proapoptotic Bax Protein expression from Liver Homogenates of Zucker Obese Rats.

Bax was analyzed by Western blot analysis as described in Materials and Methods. 50 µg of liver Protein Samples was separated by 12% SDS-PAGE gel and transferred onto PVDF membranes. The blots were blocked about 4-5 hours. The membrane was probed with primary anti-Bax and Anti- α -tubulin at a final dilution of 1:200 and 1:1000 respectively. Then secondary antibody (a goat anti-rabbit HRP conjugated) at a final dilution of 1:2500. The blots were exposed by ECL Plus substrate and developed on X-Ray film. (A) Representative western blots of Bax using 50 µg of liver protein from Zucker Obese (Ob) and Lean (Ln) rats. (B) shows densitometric quantitation $p < 0.05$ as determined by Independent-Samples T-test. Bar graph represents level of Bax protein. The standard deviations of the experiment for each group of 6 animals are shown on the bars as determined by descriptive analysis. (C) shows Normalized densitometric quantitation $p < 0.05$ as determined by Independent-Samples T-test. Bar graph represents level of Bax protein normalized to Anti- α -tubulin. The standard deviations of the experiment for each group of 6 animals are shown on the bars as determined by descriptive analysis.

(A)



(B)



(C)

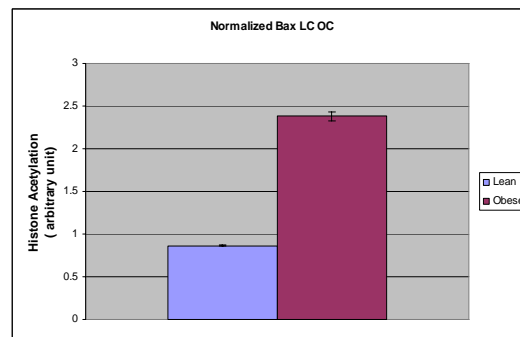
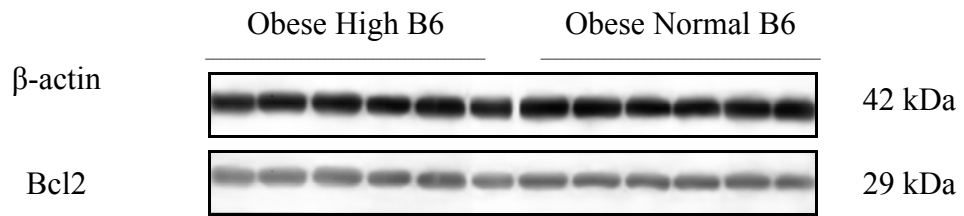


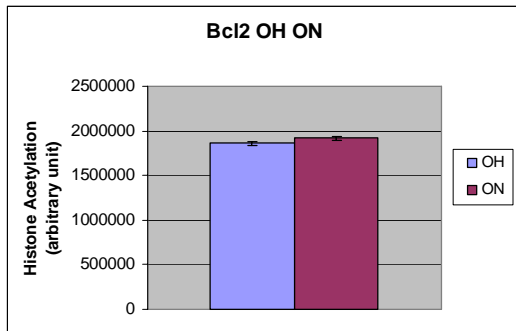
Figure 36: Western Blot Analysis of anti-apoptotic Bcl2 Protein expression from Liver Homogenates of Zucker Obese Rats.

Bcl2 was analyzed by Western blot analysis as described in Materials and Methods. 50 µg of liver Protein Samples was separated by 12% SDS-PAGE gel and transferred onto PVDF membranes. The blots were blocked about 4-5 hours. The membrane was probed with primary anti-Bcl2 and β-actin separately at a final dilution of 1:1000 and 1:2500 respectively. Then secondary antibody (a goat anti-rabbit HRP conjugated) and (a goat anti-mouse HRP conjugated) at a final dilution of 1:2500 and 1:2500 for histone and β-actin was used respectively. The blots were exposed by ECL Plus substrate and developed on X-Ray film. (A) Representative western blots of Bcl2 and β-actin using 50 µg of liver protein from Zucker Obese with high vitamin B6 (OH) and Zucker Obese with normal vitamin B6 (ON). (B) shows densitometric quantitation $p < 0.05$ as determined by Independent-Samples T-test. Bar graph represents level of Bcl2 protein of the relative intensities of Bcl2 bands. The standard deviations of the experiment for each group of 6 animals are shown on the bars as determined by descriptive analysis. (C) shows normalized densitometric quantitation $p < 0.05$ as determined by Independent-Samples T-test. Bar graph represents level of Bcl2 protein of the relative intensities of Bcl2 bands normalized to β-actin. The standard deviations of the experiment for each group of 6 animals are shown on the bars as determined by descriptive analysis.

(A)



(B)



(C)

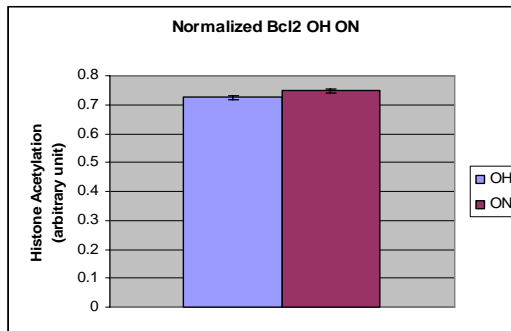
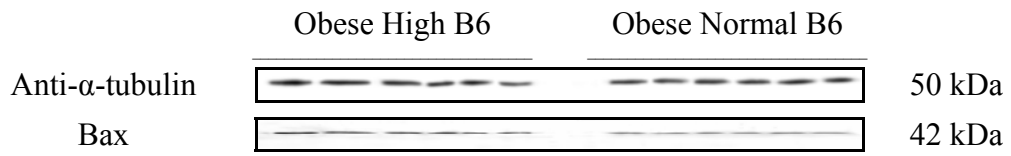


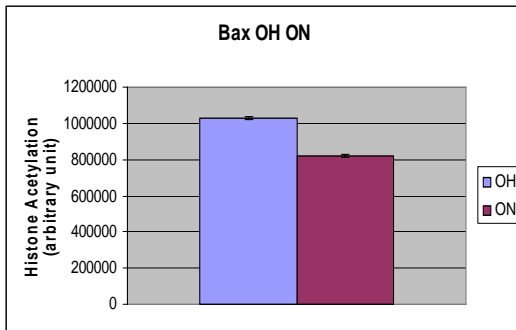
Figure 37: Western Blot Analysis of Proapoptotic Bax Protein expression from Liver Homogenates of Zucker Obese Rats.

Bax was analyzed by Western blot analysis as described in Materials and Methods. 50 µg of liver Protein Samples was separated by 12% SDS-PAGE gel and transferred onto PVDF membranes. The blots were blocked about 4-5 hours. The membrane was probed with primary anti-bax at a final dilution of 1:200, and secondary antibody (a goat anti-rabbit HRP conjugated) at a final dilution of 1:25000. The blots were exposed by ECL Plus substrate and developed on X-Ray film. (A) Representative western blots of Bax using 50 µg of liver protein from Zucker Obese with high vitamin B6 (OH) and Zucker Obese with normal vitamin B6 (ON). (B) shows densitometric quantitation $p < 0.05$ as determined by Independent-Samples T-test. Bar graph represents level of Bax protein. The standard deviations of the experiment for each group of 6 animals are shown on the bars as determined by descriptive analysis. (C) shows normalized densitometric quantitation $p < 0.05$ as determined by Independent-Samples T-test. Bar graph represents level of Bax protein normalized to Anti- α -tubulin. The standard deviations of the experiment for each group of 6 animals are shown on the bars as determined by descriptive analysis.

(A)



(B)



(C)

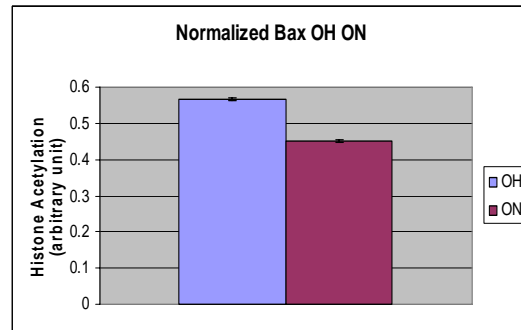
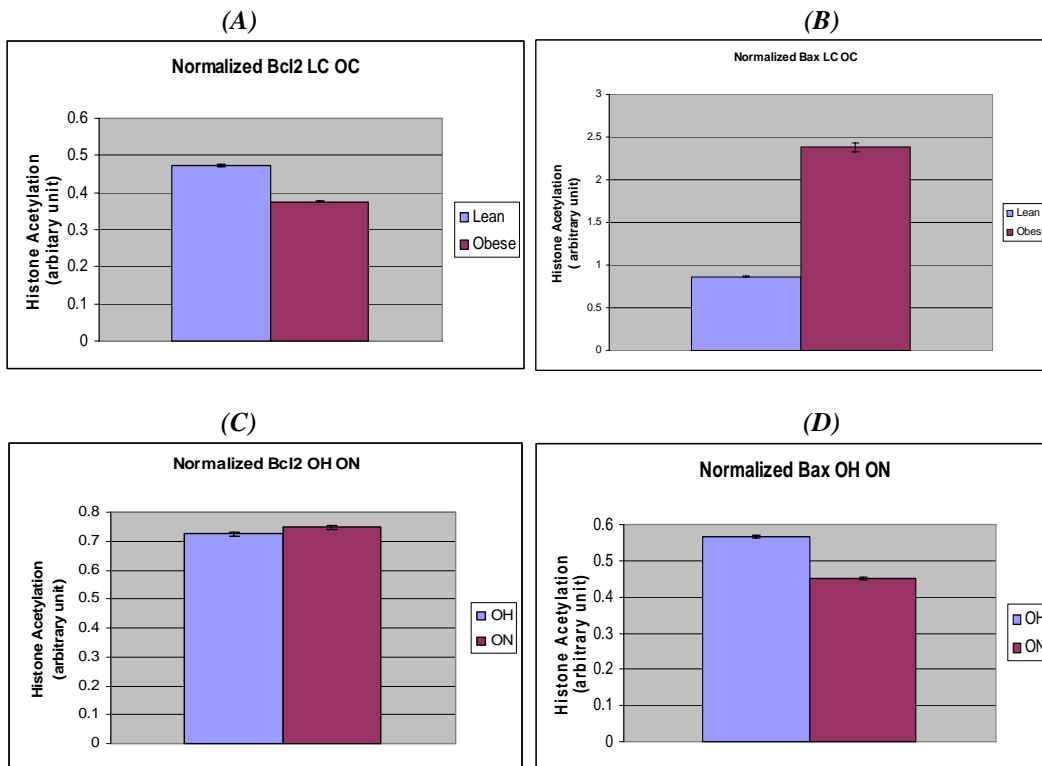


Figure 38: Summary of normalized densitometric quantitation of Bax and Bcl-2 Protein expression from Liver Homogenates of Zucker Rats.

(a) anti-Proapoptotic Bcl2 Protein expression from Liver Homogenates of Zucker Rats. (b) Proapoptotic Bax Protein expression from Liver Homogenates of Zucker Rats. (c) anti-Proapoptotic Bcl2 Protein expression from Liver Homogenates of Obese Zucker Rats. (d) Proapoptotic Bax Protein expression from Liver Homogenates of Obese Zucker Rats.



Chapter 4:

Discussion

Histone acetylation is associated with increased gene transcription [9,15] and hence with transcriptionally active chromatin domains. Histones deacetylation, on the other hand, confers repressed gene transcription [48]. Therefore, chromatin remodeling following histone acetylation or deacetylation plays a central role in the regulation of expression of many genes. Some reports show that up-regulation of inflammatory genes such as COX-2 and TNF- α involves in the pathology of a number of diseases [59,62]. However, *in vivo* histone acetylation state in disease such as hepatic steatosis is not yet known. Our present study bring a new perspective in this area. The main objective of this study was to elucidate the pattern and level of H3 and H4 acetylation both in nuclear and homogenate fractions in pathological state of hepatic steatosis and determine if hyper-acetylation can be a protective response to it. It was also of interest to assess the expression of anti-apoptotic and pro-apoptotic factor Bcl-2 and Bax in respect to histone acetylation. Investigation of histone acetylation level and pattern in Zucker obese rats, and comparison to their lean counterpart provide a new insight as to the association of acetylated state in the pathogenesis of hepatic steatosis associated with obesity.

In order to initiate the study, nuclear fraction was extracted from the liver of Zucker rats. Protein concentration was estimated and the linear range was determined in order to find appropriate protein concentration. The purity of nuclear fractions was also determined by probing membrane containing nuclear fractions against anti-tubulin antibody. Nuclear fraction was almost pure, but unfortunately, there was no positive control in order to solidify this observation. Histone 3 (H3) and histone 4 (H4) are

dominant players in chromatin fiber folding and intermolecular fiber-fiber interactions [6]; therefore H3 and H4 were selected as a good candidate to study acetylation in association with transcription.

In a previous study, enhancement in acetylation of nuclear histone H3 at lysine 9 & 14 (K9, K14) and nuclear histone H4 at K5, K8, K12 in high glucose condition, mimicking diabetes, in human monocytes THP-1 has been reported [59]. At about the same time, Hyperacetylation of H3 in amelioration of experimental colitis, which is an inflammatory disease, has been also reported [62]. It has been also believed that hepatic steatosis is in part due to oxidative stress and abundance of pro-inflammatory cytokines such as tumor necrosis factor- α (TNF- α) [69]. Furthermore, It has been shown that in human alveolar epithelial cells (A549), both TNF- α and oxidant alter histone acetylation/deacetylation, and activate NF- κ B which in turn lead to release of the pro-inflammatory cytokines [72]. Therefore, the primary objective of this research was to assess whether histone acetylation is involved and altered in Zucker obese rats which contained not only hyperglycemia and sustained inflammatory state but also exhibit steatotic liver.

The findings reported in these papers were used as a starting point for the present study. For the starting point of the experiments, all of four anti-lysine antibody for each H3 (K9, K14, K18 & K23) and H4 (K5, K8, K12, & K16) was used. Based on preliminary results and previous studies specific lysine K9, K14 for histone 3 and K5, and 12 for histone 4 was selected.

In this research project, in control lean animal versus obese, slightly lower levels of global histone H3 and H4 were found in liver homogenates and nuclear fractions in obese

animals. Evidence shows that reduced levels of global histone acetylation are associated with tumorigenesis, invasion and metastasis in gastric cancer [70]. It is also clear that acetylated histone H4 expression reduced in colorectal cancer and gastric carcinomas in comparison with nonneoplastic mucosa [71]. Our present result is proportional to these findings and opens up the possibility that sensitivity of obese rats to colon cancer as well as their proinflammatory state may take part to decrease global histone H3 and H4 acetylation.

Additionally, we obtained that obese animals had higher histone acetylation levels in liver homogenates for H3 (K9 and K14) and for H4 at K5. Histone 4 has to be mono-, di- or triacetylated at either K5, K8 and K12 in order to go into the nucleus for chromatin assembly. Unacetylated H3 would be incorporated into nucleosome by way of H4 acetylation [73]. This acetylation serve as a chemical tag to induce chromatin assembly factor 1 (CAF1) which assembles newly synthesized H3 and H4 onto replicating DNA *in vitro*. [74]. Therefore, results obtained in this study, suggest that a slight difference in global histones does not really count for the level of nuclear acetylation. In other words, higher amount of global histone will not necessarily lead to higher level of nuclear histone acetylation.

Having in mind that histone acetylation in the cytoplasm is necessary for histones' transport into nucleus; higher level of histone acetylation in liver homogenate fraction of obese animals could be explained by increased transport of histones from cytoplasm into nucleus as a response to obesity condition. The other possibility is that histones from liver homogenate of obese rats get deacetylated either immediately after entering nucleus

or upon binding to DNA, by deacetylases, which are integral part of numerous silencing complexes.

Interestingly, in nuclear fraction, histone acetylation levels were opposite to the levels noted in the whole tissue homogenate; histone acetylation levels were higher in the lean and lower in the obese animals. Neither in homogenate fractions nor in nuclear fractions, acetylation was detected for H4 at K12; but if we could have a positive control, we would be more able to rely on the results at K12.

It is still unclear whether the lower level of nuclear acetylation in obese animals in comparison with their lean counterparts has a protective role through silencing (not activating) some genes such as, for example, inflammatory genes TNF-alpha and COX-2 or it has a negative effect by turning off tumor suppressor genes. Therefore, it can be reasonable to suggest that lower acetylation of these specific lysine in nuclear hepatic fraction in obese rats may possibly correlate in the pathogenicity of hepatic steatosis as a result of obesity with hyperglycemia. More specifically H4 at lysine 5 and probably H3 at lysine 9 may probably have more effect in this process.

In addition, the levels of histone acetylation in obese animals fed five times normal vitamin B6 (OH) diet and obese animals fed normal amount of vitamin B6 (ON) were also analyzed. The animals received an AOM injection twice. It was previously found in experiment conducted in our lab (by A. Kular) that vitamin B6 has therapeutic effect and decreases the size and preneoplastic lesions in obese animals. In the present study, it was shown that in both homogenate and nuclear fractions, histone acetylation level of H3 at K9 and K14 and of H4 at K5 are higher in OH animals. This observation is in correlation with the findings reported by Glauben *et al* (2006) [62] which indicate that

hyperacetylation of histones in liver nuclei correlates with amelioration of hepatic steatosis. Therefore, we could conclude that the level of nuclear histone acetylation in OH group is more similar to lean than obese counterparts, suggesting better health conditions, including lower liver weight, size and etc, along with hyperacetylation of histone H3 and H4 at specific lysine residues.

Since Zucker obese rats are more sensitive to many diseases including diabetes, inflammatory disease and cancer [69], it was interesting to see if the levels of anti-apoptotic and pro-apoptotic proteins Bcl2 and Bax are different in obese versus lean and to assess if this difference could be correlated with hypoacetylation of histones at specific lysine residues. Oxidative stress has a significant role in the development of many human diseases, including atherosclerosis, cancer and diabetes. [75] Some of the wide range of oxidative damage within the cell can be the result of respiration and glucose metabolism which in turn generate hydroxyl radicals and other reactive oxygen species (ROS) [76]. ROS as well as hyperglycemia can trigger apoptosis pathway. Zucker obese rats can exhibit more oxidative stress because of the hyperglycemia. We hypothesized that in obese rats apoptotic pathway will be triggered due to the prolonged oxidative stress, which means they would show an increase in pro-apoptotic Bax and decrease in anti-apoptotic Bcl2, compared to their lean counterparts. This hypothesis was proven by our result which suggests that higher level of Bax and lower level of Bcl-2 may also be associated with pathological state of the tissue.

Vitamin B6 was used as anticancer treatment. It has been shown that supplemental vitamin B6 have no effect on apoptosis in colonic cell [72]. Therefore, we were expecting to have a high Bcl-2 and low Bax as in lean animals for OH group. But surprisingly,

against our expectation, obese animals fed high vitamin B6 diet had lower Bcl-2 and higher Bax expression. One possibility can be that the increased level of Bax did not become functional as an indirect effect of vitamin B6 on factor such as Bid (which makes Bax functional). The other possibility can be that therapeutic vitamin B6 possibly acted as histone deacetylase inhibitors which increased the level of histone acetylation which in turn increased the level of Bax in OH group.

In general, these results represent to our knowledge the first demonstration that nuclear hyperacetylation may probably correlate with the amelioration of hepatic colitis associated with obesity. It is also suggestive that even though apoptotic factors Bax and Bcl-2 can play a non negligible role in this process but may also be associated with pathological state of the tissue.

Appendix

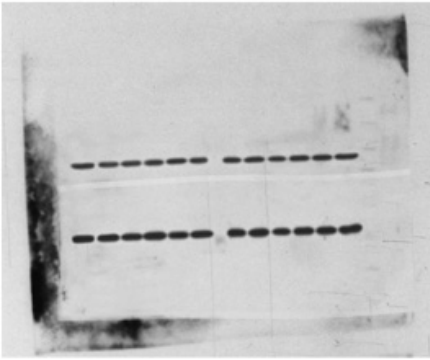


figure 04

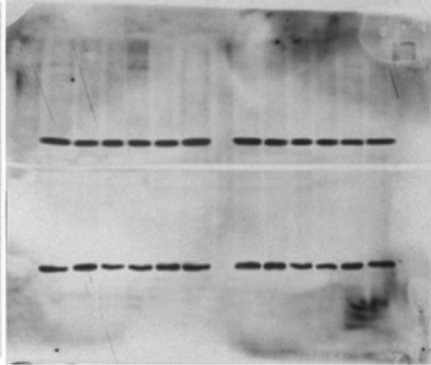


figure 05

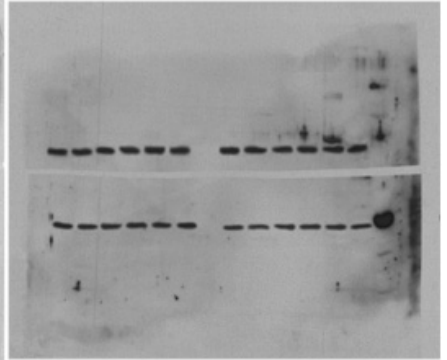


figure 06

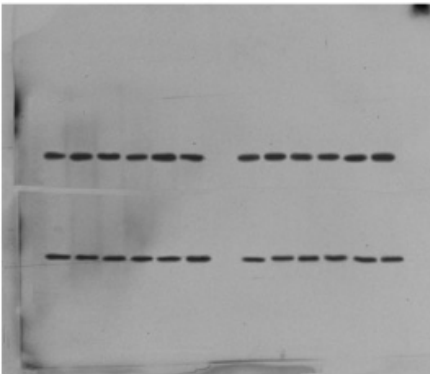


figure 07

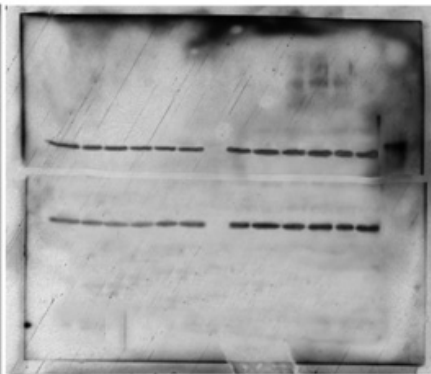


figure 09

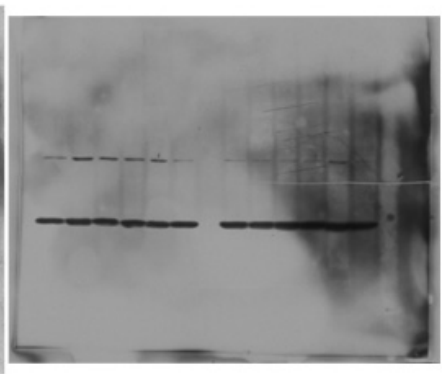


figure 10

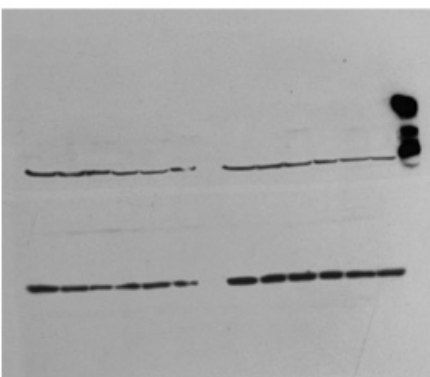


figure 11

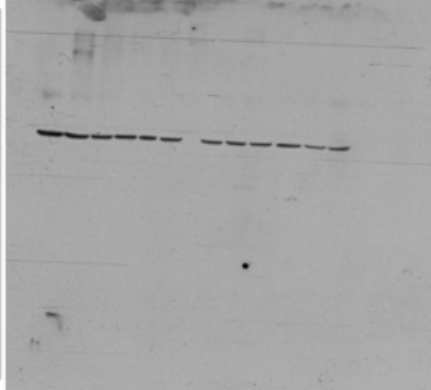


figure 12

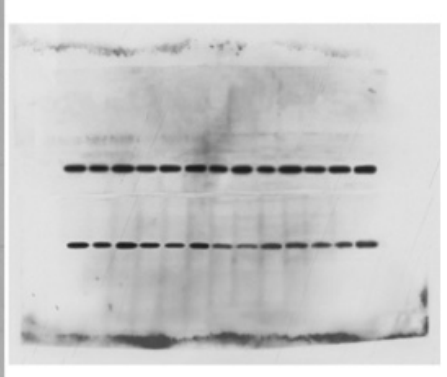


figure 14

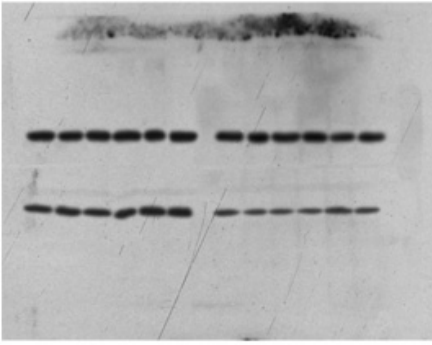


figure 15

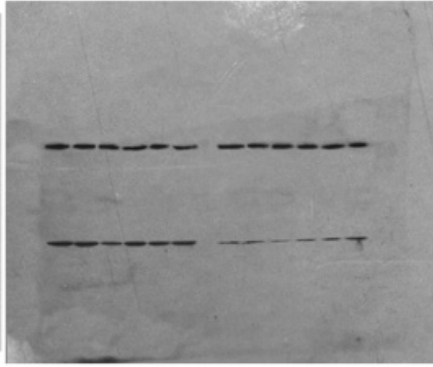


figure 16

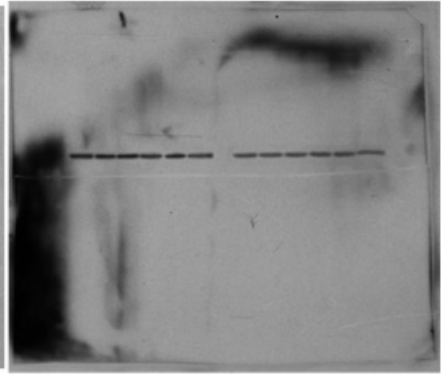


figure 17

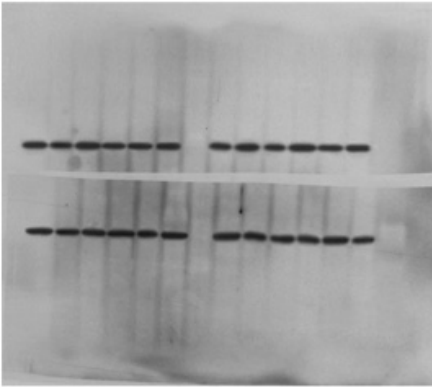


figure 19

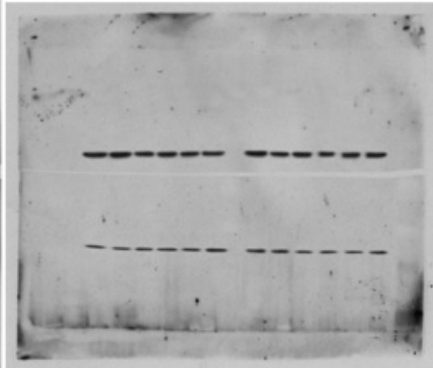


figure 20

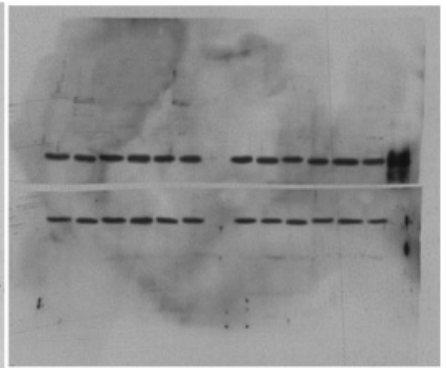


figure 21

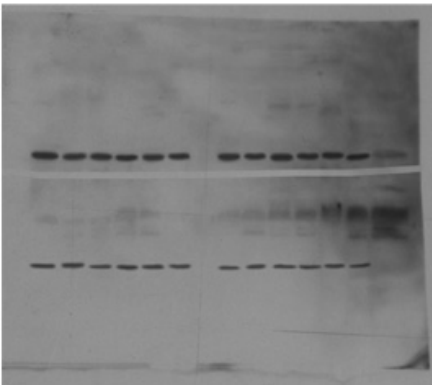


figure 22

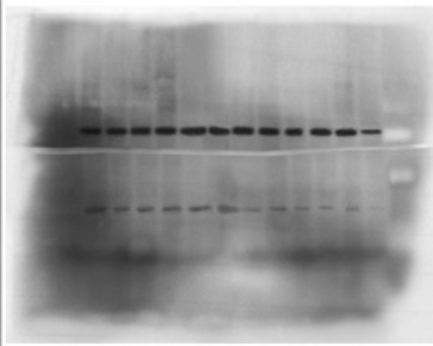


figure 24

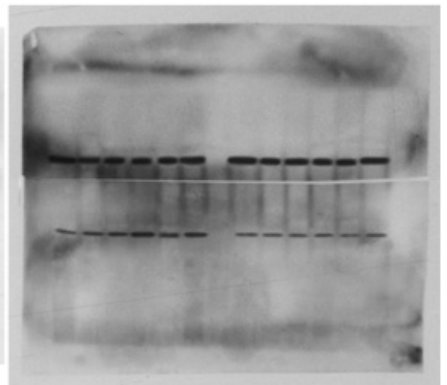


figure 25

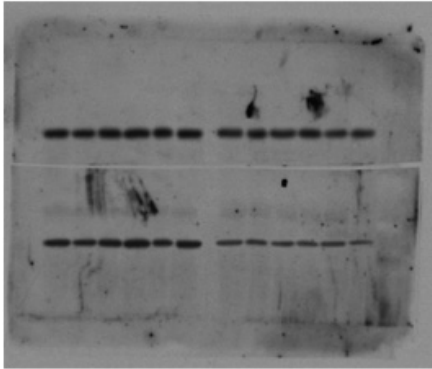


figure 26

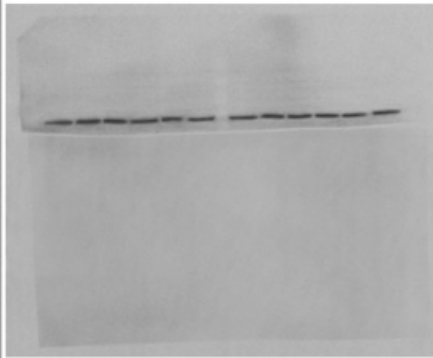


figure 27

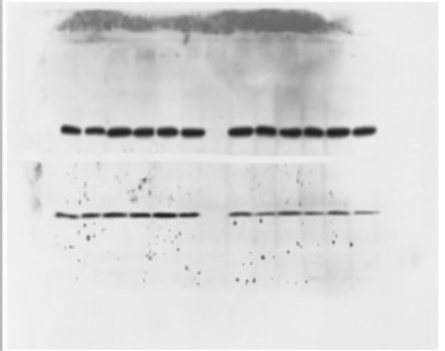


figure 29

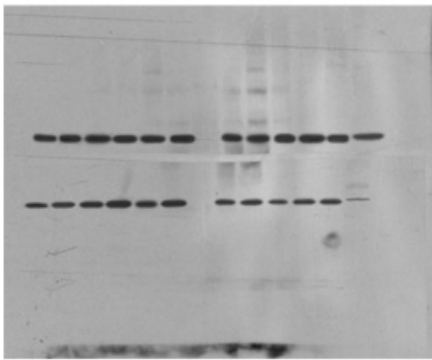


figure 30

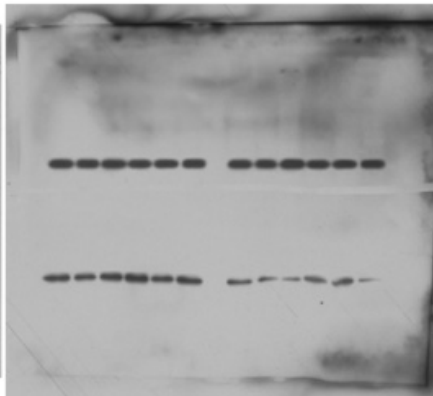


figure 31

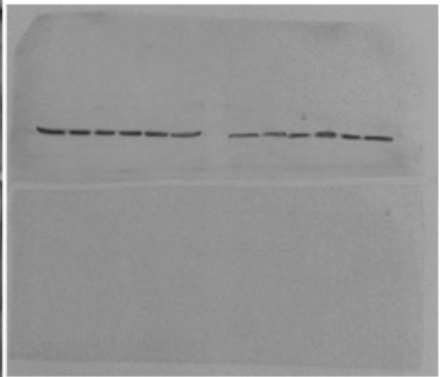


figure 32

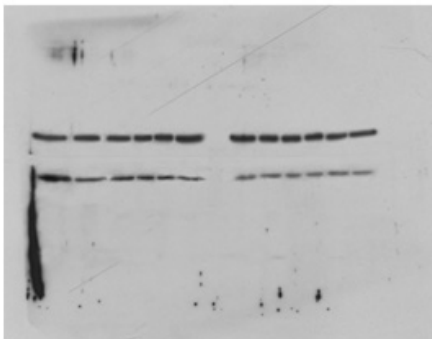


figure 34

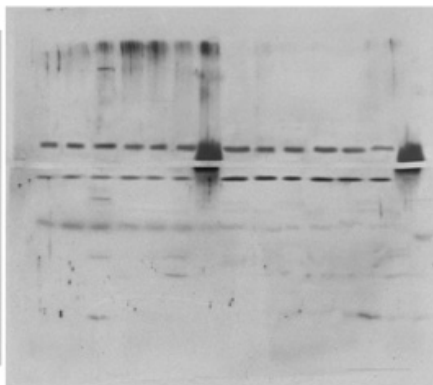


figure 35

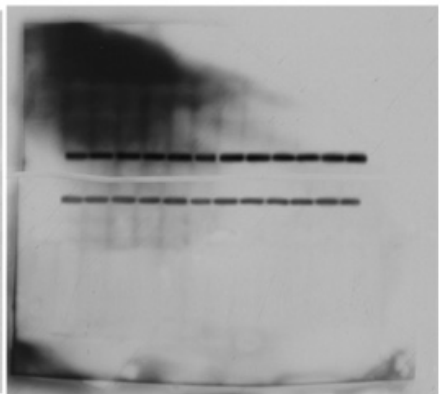


figure 36

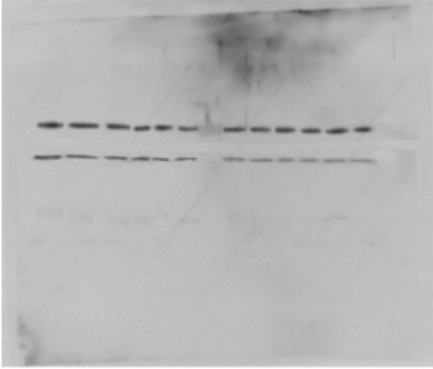


figure 37

References

- [1] Antonello Mai *et al* (2005). Histone deacetylation in epigenetics. *Medicinal Research Reviews*, **25**:261-309.
- [2] Fire A. (1998) Potent and specific genetic interference by double-stranded RNA in caenorhabditis elegans. *Nature.*, **391**:806-811.
- [3] Feinberg AP. (2001) Cancer epigenetics takes center stage. *Proc Natl Acad Sci USA.*, **98**:392-394.
- [4] Harmit S Malik, Steven Henikoff. (2003) Phylogenomics of the nucleosome. *Nat Struct Biol.* Nov;**10(11)**:882-91.
- [5] Patrick A Grant. (2001) A tale of histone modifications. *Genome Biology*, **2(4)**:reviews:0003.1-0003.6.
- [6] James R Davie. (1998) Covalent modifications of histones: expression from chromatin templates. *Current Opinion in Genetics & Development*, **8**: 173-178.
- [8] Workman, J.L. et al. (1998) Alteration of nucleosome structure as a mechanism of transcriptional regulation. *Annu. Rev. Biochem.* **67**: 545–579
- [7] V. G. Allfrey, R. Faulkner and A. E. Mirsky. (1964) Acetylation and methylation of histones and their possible role in the regulation of RNA synthesis. *Proc. Natl. Acad. Sci.*, **51**:786-794.
- [9] Struhl K. (1998) Histone acetylation and transcriptional regulatory mechanisms. *Genes Dev*, **12**:599-606.
- [10] Strahl B.D. *et al.* (2000) The language of covalent histone modifications. *Nature*, **403**:41-45.
- [11] MEI *et al.*, (2004) HDAC Inhibitors in the treatment of cancer, *International Journal of Oncology*, **25**: 1509-1519.
- [12] Jenuwein T. and Allis C.D. (2001) Translating the histone code. *Science*, **293**:1074-1080.
- [13] Turner B.M. (2000) Histone acetylation and an epigenetic code. *Bioessays*, **22**:836-845.
- [14] Brownell, J.E. *et al.* (1996) Tetrahymena histone acetyltransferase A: a homolog to yeast Gcn5p linking histone acetylation to gene activation. *Cell*, **84**: 843–851.
- [15] Hebbes T. R., Thorne A. W. and Crane-Robinson C. (1988) A direct link between core histone acetylation and transcriptionally active chromatin. *EMBO J.*, **7**: 1395-1403.
- [16] Hebbes T. R., Clayton A. L., Throne 12- Vidli G., Boffa L. C., Bradbury E. M. and Allfrey V. G. (1978) Butyrate suppression of histone deacetylation leads to accumulation of multiacetylated forms of histones H3 and H4 and increased DNAase I sensitivity of the associated DNA sequences. *Proc. Natl. Acad. Sci. USA*, **75**: 2239–2243.
- [17] A. W. and Crane-Robinson C. (1994) Core histone hyperacetylation co-maps with generalized DNase I sensitivity in the chicken beta-globin chromosomal domain. *EMBO J.*, **13**: 1823–1830.
- [18] Vettese-Dadey M., Grant P. A., Hebbes T. R., Crane-Robinson C., Allis C. D. and Workman J. L. (1996) Acetylation of histone H4 plays a primary role in enhancing transcription factor binding to nucleosomal DNA in vitro. *EMBO J.*, **15**: 2508–2518.

- [19] Durrin LK, Mann RK, Kayne PS and Grunstein M. (1991) Yeast histone h4 nterminal sequence is required for promoter activation *in vivo*. *Cell*, **65**:1023-31.
- [20] Yoshida M, Horinouchi S and Beppu T. (1995) Trichostatin a and trapoxin: novel chemical probes for the role of histone acetylation in chromatin structure and function. *Bioessays*, **17**:423-30.
- [21] Kouzarides T. (1999) Histone acetylases and deacetylases in cell proliferation. *Curr Opin Genet Dev*, **9**:40-48.
- [22] Ma, X., Wu, J., Altheim, B., Schultz, M. C. & Grunstein, M. Histone H4 acetylation sites that are required for deposition *in vivo*. Proc. Natl Acad. Sci. USA (submitted)
- [23] Janknecht, R. and T. Hunter. (1996) Transcription control: versatile molecular glue. *Curr. Biol.*, **6**:22–23.
- [24] S.Timmermann, H. Lehrmann, A. Polesskaya and A. Harel-Bellan. (2001) Histone acetylation and disease. *Cell. Mol. Life. Sci.*, **58**:728–736.
- [25] Chrivia J. C., Kwok R. P., Lamb N., Hagiwara M., Montminy M. R. and Goodman R. H. (1993) Phosphorylated creb binds specifically to the nuclear protein cbp. *Nature*, **365**:855–859.
- [26] Eckner R., Ewen M. E., Newsome D., Gerdes M., DeCaprio J. A., Lawrence J. B. *et al.* (1994) Molecular cloning and functional analysis of the adenovirus E1A-associated 300-kd protein (p300) reveals a protein with properties of a transcriptional adaptor. *Genes Dev.*, **8**:869–884.
- [27] Goodman, R. H. and S. Smolik. (2000) Cbp/p300 in cell growth transformation, and development. *Genes Dev.*, **14**:1553–1577.
- [28] E. Di Gennaro, F. Bruzzese, M. Caraglia, A. Abruzzese and A. Budillon. (2004) Acetylation of proteins as novel target for antitumor therapy. *Amino Acids*, **26**:435–441.
- [29] Hupp T. R., Meek D. W., Midgley C. A. and Lane D. P. (1992) Regulation of the specific dna binding function of p53. *Cell*, **71**:875–886.
- [30] Borrow J., Stanton V. P., Andresen J. M., Becher R., Behm F. G., Chaganti R. S. K., Civin C. I. *et al.* (1996) The translocation t(8;l6)(p11, p13) of acute myeloid leukaemia fuses a putative acetyltransferase to the creb binding protein. *Nature Genet*, **14**:33–41.
- [31] Carapeti M., Aguiar R. C. T., Watmore A. E., Goldman J. M. and Cross N. C.P. Consistent fusion of moz and tif2 in aml with inv(8)(p11q13). 1999. *Cancer Genet. Cytogenet*, **113**:70–72.
- [32] Hilfiker A., Hilfiker-Kleiner D., Pannuti A. and Lucchesi J. C. *mof.* (1997) a putative acetyltransferase gene related to the tip60 and moz human genes and to the sas genes of yeast, is required for dosage compensation in drosophila. *EMBO J.*, **16**:2054–2060.
- [33] Michael J. Carrozza, Rhea T. Utley, Jerry L. Workman and Jacques Cote. (2003) The diverse functions of histone acetyltransferase complexes. *TRENDS in Genetics*, **19 No.6**:321–329.
- [34] Brownell J.E. *et al.* (1996) Tetrahymena histone acetyltransferase a: a homolog to yeast gcn5p linking histone acetylation to gene activation. *Cell*, **84**:843–851.
- [35] Creaven M., Hans F., Mutskov V., Col E., Caron C., Dimitrov S. *et al.* (1999) Control of the histone-acetyltransferase activity of tip60 by the hiv-1 transactivator protein, tat. *Biochemistry*, **38**:8826–8830.
- [36] Brady M. E., Ozanne D. M., Gaughan L., Waite I., Cook S., Neal D. E. *et al.* (1999) Tip60 is a nuclear hormone receptor coactivator. *J. Biol. Chem.*, **274**:17599–17604.

- [37] Voegel J. J., Heine M. J., Tini M., Vivat V., Chambon P. and Gronemeyer H. (1998) The coactivator *tif2* contains three nuclear receptor-binding motifs and mediates transactivation through *cbp* binding-dependent and -independent pathways. *EMBO J.*, **17**:507–519.
- [38] Yao T. P., Ku G., Zhou N., Scully R. and Livingston D. M. (1996) The nuclear hormone receptor coactivator *src-1* is a specific target of *p300*. *Proc. Natl. Acad. Sci. USA*, **93**:10626–10631.
- [39] Robin X. Luo and Douglas C. Dean. (1999) Chromatin remodeling and transcriptional regulation. *J Natl Cancer Inst*, **91**:1288–1294.
- [40] Murata T, Kurokawa R and Kronen A. (2001) Defect of histone acetyltransferase activity of the nuclear transcriptional coactivator *cbp* in rubinstein-taybi syndrome. *Hum Mol Genet*, **10**:1071–1076.
- [41] Muraoka M., Konishi M., Kikuchi-Yanoshita R., Tanaka K., Shitara N., Chong J. M. *et al.* (1996) *p300* gene alterations in colorectal and gastric carcinomas. *Oncogene*, **12**:1565–1569.
- [42] Liu L., Scolnick D. M., Trievel R. C., Zhang H. B., Marmorstein R., Halazonetis T. D. *et al.* (1999) *p53* sites acetylated *in vitro* by *pcaf* and *p300* are acetylated *in vivo* in response to dna damage. *Mol. Cell Biol.*, **19**:1202–1209.
- [43] Sakaguchi K., Herrera J. E., Saito S., Miki T., Bustin M., Vassilev A. *et al.* (1998) Dna damage activates *p53* through a phosphorylation- acetylation cascade. *Genes Dev.*, **12**:2831–2841.
- [44] Egan C., Jelsma T. N., Howe J. A., Bayley S. T., Ferguson B. and Branton P. E. (1988) Mapping of cellular protein-binding sites on the products of early-region 1a of human adenovirus type 5. *Mol. Cell Biol.*, **8**:3955–3959.
- [45] Gray SG and Ekstrom TJ. (2001) The human histone deacetylase family. *Exp cell cs*, **262**:75-83.
- [46] Shaowen Wang, Yan Yan-Neale, Marija Zeremski and Dalia Cohen. (2004) Transcription regulation by histone deacetylases.
- [47] Robin X. Luo, Douglas C. Dean. (1999) Chromatin Remodeling and Transcriptional Regulation. 1999. *J Natl Cancer Inst*, **91**:1288–94.
- [48] Boffa LC, Vidali G, Mann RS and Allfrey VG. (1978) Suppression of histone deacetylation *in vivo* and *in vitro* by sodium butyrate. *J Biol Chem*, **253**: 3364-3366.
- [49] Candido EP, Reeves R and Davie JR (1978) Sodium butyrate inhibits histone deacetylation in cultured cells. *Cell*, **14**: 105-113.
- [50] Blaheta RA, Nau H, Michaelis M and Cinatl J Jr. (2002) Valproate and valproate-analogues: potent tools to fight against cancer. *Curr Med Chem*, **9**: 1417-1433.
- [51] Gore SD and Carducci MA (2000) Modifying histones to tame cancer: clinical development of sodium phenylbutyrate and other histone deacetylase inhibitors. *Expert Opin Investig Drugs* **9**: 2923-2934.
- [52] Van Lint C, Emiliani S, Verdin E. (1996) The expression of a small fraction of cellular genes is changed in response to histone hyperacetylation. *Gene Expr*, **5**: 243–253.
- [53] Yoshida M, Kijima M, Akita M and Beppu T. (1990) Potent and specific inhibition of mammalian histone deacetylase both *in vivo* and *in vitro* by trichostatin A. *J Biol Chem*, **265**: 17174-17179.
- [54] Lockshin. (1964) Programmed cell death—II. Endocrine potentiation of the breakdown of the intersegmental muscles of silkworms. *Journal of Insect Physiology* **10**: 643-649.

- [55] Kerr JF WA, C. A. (1972) Apoptosis: A basic biological phenomenon with wide-ranging implications in tissue kinetics. *Br J Cancer*, **26**: 239-257.
- [56] Saikumar, P., Dong, Z., Mikhailov, V., Denton, M., Weinberg, J.M., and Venkatachalam, M.A. (1999) Apoptosis: definition, mechanisms, and relevance to disease. *Am J Med*, **107**: 489-506.
- [57] Luo, X., Budihardjo, I., Zou, H., Slaughter, C., and Wang, X. (1998) Bid, a Bcl2 interacting protein, mediates cytochrome c release from mitochondria in response to activation of cell surface death receptors. *Cell*, **94**: 481-490.
- [58] Vincenzo Chiarugi, Lucia Magnelli and Marina Cinelli (1997) Complex Interplay Among Apoptosis Factors: RB, P53, E2F, TGF- β , Cell Cycle Inhibitors and the bcl2 Gene Family, *Pharmacological Research*, **Vol. 35, No. 4**: 257-261
- [59] Feng Miao, Irene Gaw Gonzalo, Linda Lanting, and Rama Natarajan. (2004) In Vivo Chromatin Remodeling Events Leading to Inflammatory Gene Transcription under Diabetic Conditions. *J. Biol. Chem.*, **Vol. 279, Issue 17**, 18091-18097.
- [60] Guha, M., Bai, W., Nadler, J. L., Natarajan, R. (2000) Molecular Mechanisms of Tumor Necrosis Factor alpha Gene Expression in Monocytic Cells via Hyperglycemia-induced Oxidant Stress-dependent and -independent Pathways. *J. Biol. Chem.* **275**: 17728-17739.
- [61] Shanmugam N, Reddy MA, Guha M, Natarajan R. (2003) High glucose-induced expression of proinflammatory cytokine and chemokine genes in monocytic cells. *Diabetes* **52**:1256–1264.
- [62] Rainer Glaben, Arvind Batra, Inka Fedke, Martin Zeitz, Hans A. Lehr, Flavio Leoni, Paolo Mascagni, Giamila Fantuzzi, Charles A. Dinarello, and Britta Siegmund. (2003) Histone Hyperacetylation Is Associated with Amelioration of Experimental Colitis in Mice. *The Journal of Immunology*, 176: 5015–5022.
- [63] Mishra, N. C., M. Reilly, D. R. Brown, P. Ruiz, and G. S. Gilkeson. (2003) Histone deacetylase inhibitors modulate renal disease in the MLR-lpr/lpr mouse. *J. Clin. Invest.* **111**: 539–552.
- [64] Leoni, F., A. Zaliani, G. Bertolini, G. Porro, P. Pagani, P. Pozzi, G. Dona, G. Fossati, S. Sozzani, T. Azam, *et al.* (2002) The antitumor histone deacetylase inhibitor suberoylanilide hydroxamic acid exhibits antiinflammatory properties via suppression of cytokines. *Proc. Natl. Acad. Sci. USA*, **99**: 2995–3000.
- [65] Baglioni S, Genuardi M. (2004) Simple and complex genetics of colorectal cancer susceptibility. *Am J Med Genet.* **15;129C(1)**:35-43.
- [66] Giovannucci E. (2003) Diet, body weight, and colorectal cancer: a summary of the epidemiologic evidence. *Women's Health (Larchmt)*, **12(2)**:173-82.
- [67] Bird RP, Yao K, Lasko CM, Good CK, (1996) Inability of low- or high-fat diet to modulate late stages of colon carcinogenesis in Sprague-Dawley rats. *Cancer res.*, **56(13)**: 2896-9.
- [68] Abu-Abid S., Szold A., Klausner J. (2002) Obesity and cancer. *J Med.*, **33 (1-4)**:73-86.
- [69] Raju J., Bird R.P. (2006) Alleviation of hepatic steatosis accompanied by modulation of plasma and liver TNF-alpha levels by *Trigonella foenum graecum* (fenugreek) seeds in Zucker obese (fa/fa) rats. *Int J Obes (Lond)*. 1-10
- [70] Yasui *et al.*: (2003) Histone acetylation gastric carcinogenesis. *Ann. N.Y. Sci.* **983**: 220-231

- [71] Ono, S., N. Oue, H. Kuniyasu, *et al.* (2002) Acetylated histone H4 is reduced in human gastric adenomas and carcinomas. *J Exp. Clin. Cancer Res.* **21**: 377-382
- [72] Rahman I. (2002) Oxidative stress, transcription factors and chromatin remodeling in lung inflammation. *Biochemical Pharmacology* **64**: 935-942
- [73] Mishael Grunstein. (1997) Histone acetylation in chromatin structure and transcription. *Nature*, **389**: 349-352
- [74] Kaufman, P. D. *et al.* (1995) The p150 and p60 subunits of chromatin assembly factor I: a molecular link between newly synthesized histone and DNA replication. *Cell*, **81**: 1105-1114
- [75] Weisel, T. *et al.* (2006) *biotechnology journal.* **1**:388-397
- [76] Vlako, M. *et al.* (2006) Free radicals, metals and antioxidants in oxidative stress induced cancer. *Chemico-biological interactions.* **160**:1-40